© 2017. Published by The Company of Biologists Ltd | Development (2017) 144, 3917-3931 doi:10.1242/dev.145698

STEM CELLS AND REGENERATION

RESEARCH ARTICLE

The E2A splice variant E47 regulates the differentiation of projection neurons via p57(KIP2) during cortical development

Sabrina Pfurr[1,2,‡], Yu-Hsuan Chu[1,2,‡], Christian Bohrer[1,2], Franziska Greulich[3], Robert Beattie[4,*], Könül Mammadzada[1,2], Miriam Hils[2,5], Sebastian J. Arnold[6,7], Verdon Taylor[4], Kristina Schachtrup[2,5], N. Henriette Uhlenhaut[3] and Christian Schachtrup[1,§]

ABSTRACT

During corticogenesis, distinct classes of neurons are born from progenitor cells located in the ventricular and subventricular zones, from where they migrate towards the pial surface to assemble into highly organized layer-specific circuits. However, the precise and coordinated transcriptional network activity defining neuronal identity is still not understood. Here, we show that genetic depletion of the basic helix-loop-helix (bHLH) transcription factor E2A splice variant E47 increased the number of Tbr1-positive deep layer and Satb2-positive upper layer neurons at E14.5, while depletion of the alternatively spliced E12 variant did not affect layer-specific neurogenesis. While ChIP-Seq identified a big overlap for E12- and E47-specific binding sites in embryonic NSCs, including sites at the cyclin-dependent kinase inhibitor (CDKI) *Cdkn1c* gene locus, RNA-Seq revealed a unique transcriptional regulation by each splice variant. E47 activated the expression of the CDKI *Cdkn1c* through binding to a distal enhancer. Finally, overexpression of E47 in embryonic NSCs *in vitro* impaired neurite outgrowth, and overexpression of E47 *in vivo* by *in utero* electroporation disturbed proper layer-specific neurogenesis and upregulated p57(KIP2) expression. Overall, this study identifies E2A target genes in embryonic NSCs and demonstrates that E47 regulates neuronal differentiation via p57(KIP2).

KEY WORDS: Basic helix-loop-helix transcription factor, Cell cycle regulation, Cortical neurogenesis, Neurite outgrowth, p57(KIP2), Enhancer, E2A

INTRODUCTION

The mammalian cerebral cortex is a complex six-layered structure whose cellular composition and organization underlies our highest cognitive, perceptual and motor functions. During cortical development, multipotent embryonic neural stem cells (NSCs), also referred to as radial glia (RG) cells, span the width of the brain wall, retaining their cell bodies in the ventricular zone (VZ) (Pinto and Gotz, 2007). RG cells undergo neurogenic asymmetric divisions to generate a proliferating RG and a more differentiated cell, either a neuron or a basal intermediate progenitor (IP). Immature neurons migrate out of the VZ where they become functionally integrated mature neurons and contribute to outer layer formation, while IPs migrate into the subventricular zone (SVZ) and proliferate to amplify the neurogenic population. RG and IP cells give rise to six cortical layers in an 'inside out' order, from the deepest layer VI, which contains early-born neurons, to layer II, which is populated by the latest born neurons (Molyneaux et al., 2007). During brain development, specification of neuronal identity is orchestrated by the sequential expression of genes that control proliferation, cellular migration and neuronal differentiation (Kwan et al., 2012; Molyneaux et al., 2015; Telley et al., 2016).

Basic helix-loop-helix (bHLH) transcription factors (TFs) play key roles in self-renewal and fate determination of NSCs during corticogenesis (Imayoshi and Kageyama, 2014; Lee, 1997; Ross et al., 2003; Vetter, 2001). bHLH TFs are characterized by a highly conserved helix-loop-helix domain comprising two amphipathic α-helices separated by a loop of variable length, which mediates the formation of homo- or heterodimers (Murre et al., 1994). This family of TFs contains a second motif of mainly basic amino acid residues that allows DNA binding to a consensus hexanucleotide E box sequence (CANNTG) (Murre et al., 1994; Voronova and Baltimore, 1990). Class I bHLH TFs, called E proteins, have the ability to function as heterodimers with class II bHLH proteins, including members of the achaete-scute [e.g. Mash1 (Ascl1)], neurogenin (Ngn1 and Ngn2) and NeuroD families (e.g. NeuroD1), for controlling differentiation and specification of NSCs and IPs during embryonic development (Lee, 1997; Wang and Baker, 2015).

E proteins are encoded by three genes, namely *Tcf3* (E2A), *Tcf4* (E2-2) and *Tcf12* (HEB). The *Tcf3* gene codes for the alternative splice variants E12 and E47. Beside its heterodimer activity with proneural TFs, E2A can interact with TFs from the Ets and Pax families and, particularly E47, has been demonstrated to act as a homodimer during B cell development (Shen and Kadesch, 1995). E2A target genes during cortical development are unknown; however, it has been demonstrated that it regulates cell cycle progression through activation of cyclin-dependent kinase inhibitors (CDKI), and cadherin-mediated cell adhesion through transcriptional repression of E-cadherin (Pagliuca et al., 2000; Pérez-Moreno et al., 2001; Prabhu et al., 1997; Rothschild et al., 2006). Differential E protein expression patterns during brain development and exclusive E2A expression in adult NSCs of the SVZ stem cell niche suggests that E proteins act during orchestration

[1]Institute of Anatomy and Cell Biology, Faculty of Medicine, University of Freiburg, Freiburg 79104, Germany. [2]Faculty of Biology, University of Freiburg, Freiburg 79104, Germany. [3]Helmholtz Diabetes Center (HDC) and German Center for Diabetes Research (DZD), Helmholtz Zentrum München, Neuherberg 85764, Germany. [4]Department of Biomedicine, Embryology and Stem Cell Biology, University of Basel, Basel 4058, Switzerland. [5]Center for Chronic Immunodeficiency (CCI), Medical Center – University of Freiburg, Faculty of Medicine, University of Freiburg, Freiburg 79106, Germany. [6]Institute of Experimental and Clinical Pharmacology and Toxicology, Faculty of Medicine, University of Freiburg, Freiburg 79104, Germany. [7]BIOSS Centre of Biological Signalling Studies, Albert-Ludwigs-University, Freiburg 79104, Germany.
*Present address: Developmental Neurobiology, IST Austria (Institute of Science and Technology Austria), Klosterneuburg 3400, Austria.
‡These authors contributed equally to this work

§Author for correspondence (christian.schachtrup@anat.uni-freiburg.de)

C.S., 0000-0001-9851-6299

Received 12 October 2016; Accepted 11 September 2017

Development (2017) 144, 3917-3931 doi:10.1242/dev.145698

of early cortical developmental processes (Bohrer et al., 2015; Ravanpay and Olson, 2008; Roberts et al., 1993). Initial generation and characterization of the E2A splice variant E12 and E47 knockout mice revealed that these splice variants fulfill distinct functions in B cell lineage specification (Beck et al., 2009). However, the precise contributions of these E2A splice variants and their target genes to cortical neurogenesis and specification of neural subtype identities is not known.

Here, we have identified the CDKI gene *Cdkn1c* as a functional target of E2A during neurogenesis. E47-deficient mouse embryos had an increase in the number of cortical plate neurons at E14.5, despite equal cell cycle progression of NSCs. Overexpression of E47 in embryonic NSCs led to upregulation of *Cdkn1c* mRNA and inhibition of neuronal differentiation. Upon E47 overexpression *in vivo* by *in utero* electroporation, p57 (KIP2) protein abundance was increased in cortical precursor cells and neuronal localization as well as neurite outgrowth was impaired. Our results suggest that the E2A splice variant E47 controls neurogenesis via the CDKI p57(KIP2) as an E47-regulated key factor in neuronal specification.

RESULTS

The E2A splice variants E12 and E47 exhibit comparable spatiotemporal expression patterns during cortical development

To investigate the role of the E2A splice variants E12 and E47 in embryonic NSCs during cortical development (Fig. 1A), we first examined the temporal expression of E2A around the peak of cortical neurogenesis. *In situ* RNA hybridization analysis showed *Tcf3* expression in cells located in the VZ and SVZ of the cortex at embryonic day 14.5 (E14.5) (Fig. S1A), consistent with expression by mitotic embryonic NSCs and progenitors. Quantitative PCR for the E2A splice variants E12 and E47 on FACS-sorted NSCs (Hes5::eGFP sorted NSCs) of different developmental stages (E11.5, E15.5 and E18.5) showed highest expression of both splice variants at E15.5 (Fig. 1B). Immunolabeling for E2A protein at E14.5 showed variegated E2A expression levels in distinct cell populations in the developing cortex (Fig. 1C). E2A was expressed by Pax6^{+} cells, separating this cell population into either high or low E2A-expressing progenitors, with higher E2A expression in Pax6^{+} cells in the apical region of the VZ (Fig. 1D). Most *Eomes*$^{GFP+}$ (Eomes,

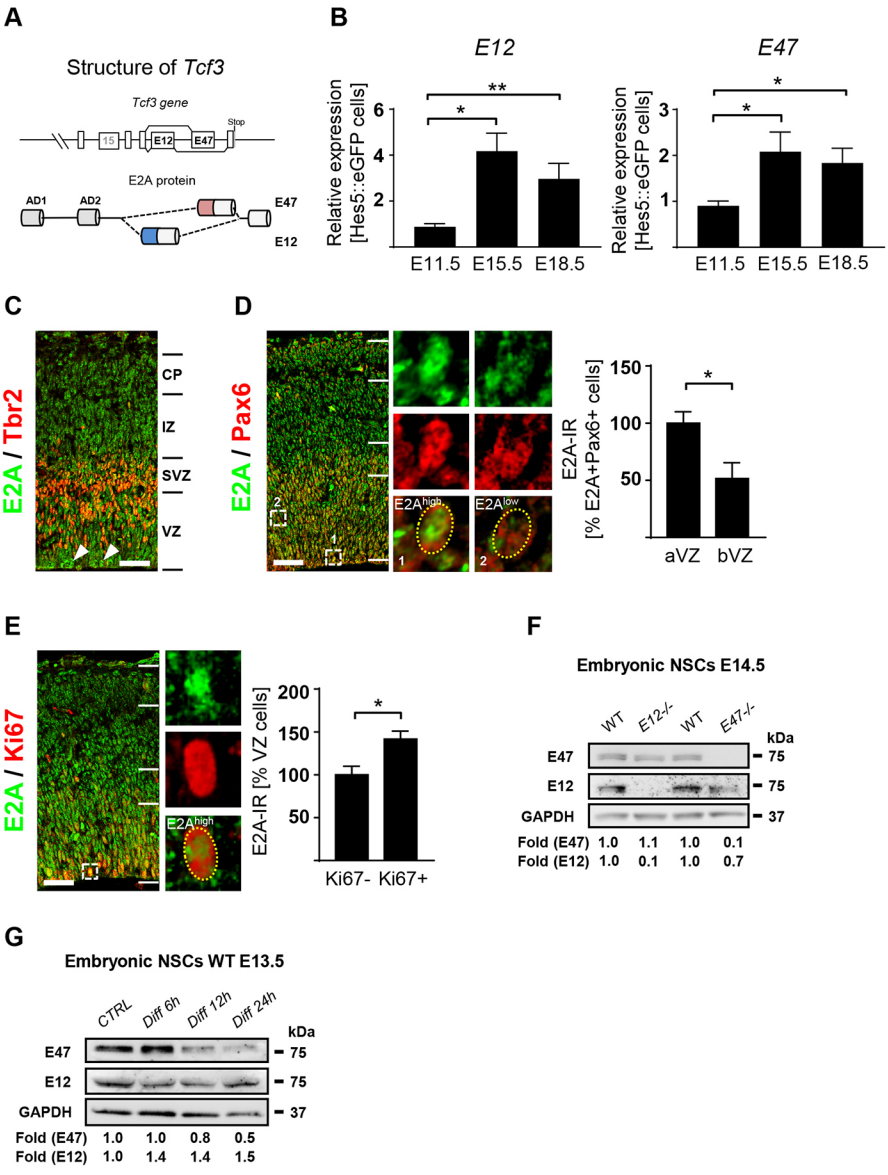

Fig. 1. Expression of the E2A splice variants E12 and E47 in the developing cortex. (A) Structure of the *Tcf3* locus. The alternatively spliced E12 and E47 proteins differ only in their DNA-binding region. (B) Expression of the E2A splice variants E12 and E47 in FACS-isolated neural stem cells at embryonic days 11.5, 15.5 and 18.5 in HES5::eGFP mice. Results are from at least three independent experiments performed in duplicate. (C) Immunolabeling for E2A (green) and Tbr2 (red) in the cortex in representative sagittal brain sections of C57BL/6 mice at E14.5. Arrowheads depict high E2A-expressing cells in the VZ. Scale bar: 45 µm. (n=3). (D,E) Immunolabeling for E2A (green) in combination with Pax6 (D, red) or Ki67 (E, red) in sagittal brain sections of mice at E14.5. White boxes indicate representative E2A colocalization with Pax6^{+} (D) and Ki67^{+} (E) cells (high magnification images are on the right). The graphs show quantification of E2A immunoreactivity per total E2A^{+}Pax6^{+} cells in the apical and basal VZ (D, right) or in E2A^{+}Ki67^{+} cells in the VZ (E, right). Scale bars: 45 µm. (n=3). (F) Immunoblot protein expression analysis for E47 and E12 in embryonic wild-type, E12$^{-/-}$ and E47$^{-/-}$ NSCs cultured under proliferation conditions. Representative western blots are shown from two (E12) and three (E47) independent experiments. (G) Immunoblot protein expression analysis for E47 and E12 in embryonic wild-type NSCs cultured under proliferation and differentiation conditions. Representative western blots are shown from six independent experiments. **P<0.01, *P<0.05 by one-way ANOVA (B) and Student's t-test (D,E). CP, cortical plate; IZ, intermediate zone; SVZ, subventricular zone; VZ, ventricular zone; aVZ, apical region of VZ; bVZ, basal region of VZ.

Development (2017) 144, 3917-3931 doi:10.1242/dev.145698

also referred to as Tbr2) IPs and Tuj-1^{+} immature neurons showed a moderate level of E2A expression (Fig. S1B,C), suggesting that E2A levels might decrease in differentiating cells. Accordingly, high E2A expression coincided with proliferating Ki67^{+} cells in the VZ (Fig. 1E), indicating a role for E2A in embryonic NSC maintenance and differentiation. In addition, high E2A expression was also observed in some cells of the upper layer of the cortical plate (Fig. S1B,C). To elucidate the specific protein abundance of the E2A splice variants E12 and E47, we first performed western blotting on E12$^{-/-}$ and E47$^{-/-}$ NSCs to confirm antibody specificity (Fig. 1F). The E12 protein abundance increased, while the E47 protein abundance decreased during the temporal progress of embryonic NSC differentiation (Fig. 1G), suggesting that both splice variants might differently regulate neuronal differentiation of precursor cells in the VZ and SVZ.

E47 deficiency leads to increased numbers of Tbr1^{+} and Satb2^{+} neurons, while E12 has no effect on cortical neurogenesis

To study the functions of the E2A splice variants E12 and E47 in the developing cortex, we examined the impact of splice variant-specific loss of function on the specification of NSCs and their progeny. Detailed cortical layer analysis at E14.5 revealed a significant increase in the total number of Tbr1^{+} [layer VI; E47$^{-/-}$, 1.52±0.18-fold (±s.e.m.); P<0.05: Fig. 2A,C] and Satb2^{+} [layer II-V; E47$^{-/-}$, 1.6±0.06-fold (±s.e.m.); P<0.01: Fig. 2B,D] neurons in E47$^{-/-}$ embryos compared with wild-type embryos. The number of Tbr1^{+} neurons was also significantly, albeit not as drastically, increased at E18.5; at postnatal day 3 (P3) there was no significant difference in the number of Tbr1^{+} cells in E47$^{-/-}$ embryos compared with wild-type embryos (Fig. S2A-D), while the total number of Satb2^{+} early-born neurons was similar at E18.5 and P3 in E47$^{-/-}$ embryos compared with wild-type embryos (Fig. S2E,F and data not shown). E12$^{-/-}$ embryos showed no difference in Tbr1^{+} and Satb2^{+} cells compared with littermate controls at E14.5 (Fig. S2G-J), suggesting that specifically E47 controls neuronal identities. Bin analysis showed an equal increase in the number of Tbr1^{+} neurons located in bins 1 to 5 in E47$^{-/-}$ embryos compared with control (Fig. 2E), illustrating that the increase in Tbr1^{+} cells in E47$^{-/-}$ animals is not due to a shift in the localization of early-born neurons. Interestingly, Ctip2^{+} cells, which represent subcortical projection neurons of layer V, were not affected in E47$^{-/-}$ embryos

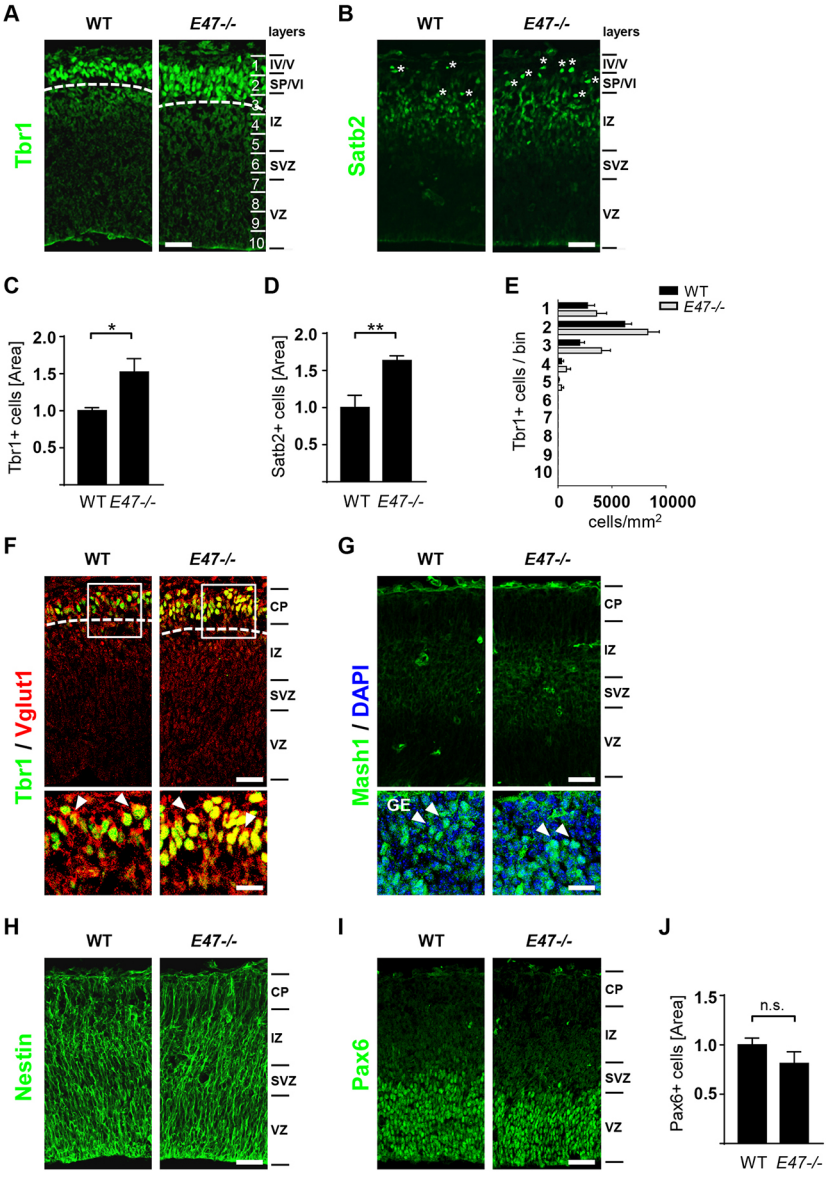

Fig. 2. E47 regulates Tbr1^{+} and Satb2^{+} neurogenesis at E14.5. (A,B) Immunolabeling for Tbr1 (A, green) and Satb2 (B, green) in sagittal brain sections of E47$^{-/-}$ mice compared with wild-type littermates at E14.5. The radial extent of the cortical wall was divided into 10 bins of equivalent height. Scale bars: 40 µm. (C,D) Quantification of the number of Tbr1^{+} (C) and Satb2^{+} (D) neurons (n=5 wild-type mice, n=4 E47$^{-/-}$ mice, C; n=5 wild-type mice, n=6 E47$^{-/-}$ mice, D). (E) Quantification of Tbr1^{+} cells located in each of 10 bins throughout the cortex in sagittal sections of E47$^{-/-}$ mice and wild-type littermates at E14.5 (n=4 mice). (F,G) Immunolabeling for Vglut1 (red) in combination with Tbr1 (green) (F), or immunolabeling for Mash1 (green) (G) in representative sagittal brain sections of E47$^{-/-}$ mice compared with wild-type littermates at E14.5. Nuclei are stained with DAPI (blue). Scale bars: 40 µm, top; 17 µm, bottom. n=3 mice. (H) Immunolabeling for nestin (green) in the cortex in representative sagittal sections of E47$^{-/-}$ mice compared with wild-type littermates at E14.5. Scale bar: 40 µm. n=4 mice. (I) Immunolabeling for Pax6 (green) in sagittal sections of E47$^{-/-}$ mice compared with wild-type littermates at E14.5. Scale bar: 40 µm. (J) Quantification of the number of Pax6^{+} radial glial cells in cortical brain sections of E47$^{-/-}$ mice and wild-type littermates at E14.5 (n=4 wild-type mice, n=3 E47$^{-/-}$ mice). Data are mean±s.e.m. **P<0.01; *P<0.05 using Student's t-test. CP, cortical plate; GE, ganglionic eminence; IV/V, cortical layer IV/V; IZ, intermediate zone; SP, subplate; SVZ, subventricular zone; VI, cortical layer VI; VZ, ventricular zone.

Development (2017) 144, 3917-3931 doi:10.1242/dev.145698

compared with wild-type littermates, suggesting that E47 regulates neurogenesis of distinct populations of excitatory cortical neurons (Fig. S2K,L). bHLH TF Ngn1 and Ngn2 have been shown to specify the properties of early-born neurons and *Ngn* mutants reveal a global shift of neuronal phenotype from cortical, glutamatergic to subcortical, GABAergic neurons (Schuurmans et al., 2004). As E47 has the ability to function as heterodimer with class II bHLH proteins, including Ngn1 and Ngn2, we analyzed whether E47 depletion results in identity changes of $Tbr1^+$ neocortical neurons. Immunolabeling for Vglut1, a marker for glutamatergic neurons, and Math2, a TF expressed by cortical neurons, revealed that the population of $Tbr1^+$ cells in $E47^{-/-}$ mice had not changed its identity (Fig. 2F and data not shown). Mash1 protein levels were strongly upregulated in *Ngn2* mutants (Schuurmans et al., 2004). In contrast, Mash1 expression was almost absent in the cortex and was not further upregulated in $E47^{-/-}$ brain sections (Fig. 2G). $Tbr1^+$ neurons are the source of $neurofilament^+$ corticothalamic axons (Bedogni et al., 2010) and, in accordance with no identity change of $Tbr1^+$ neurons in $E47^{-/-}$ mice, they appeared with normal shape (Fig. S2M,N). E2A splice variants are thought to be an essential heterodimerization partner of the proneural bHLH TFs Mash1 and Ngn2 to facilitate DNA binding. *Ngn2;Mash1* double-mutant embryos have a severe disruption of the cortical cytoarchitecture (Nieto et al., 2001). However, neither $E47^{-/-}$ nor $E12^{-/-}$ embryos had any overt differences in RG cell organization and cortex cytoarchitecture compared with wild type, as shown by immunolabeling for nestin (Fig. 2H; Fig. S2O). Furthermore, quantification of $Pax6^+$ or $Sox2^+$ RG cells in $E47^{-/-}$ embryos and $Pax6^+$ RG cells in $E12^{-/-}$ embryos revealed no significant differences compared with wild-type controls (Fig. 2I,J; Fig. S2P-S). Loss of E47 did not significantly alter the $Tbr2^+$ and $Ngn2^+$ IPs and neurogenic cell population, respectively, nor did it affect the differentiation of $NeuN^+$ neurons or apoptosis at E14.5 (Fig. S3) and E18.5 (data not shown, cleaved caspase 3). Overall, these results reveal that E47 controls the number of $Tbr1^+$ and $Satb2^+$ neurons at E14.5.

E2A binds to a variety of genes controlling cortical brain development

To identify E2A target genes during cerebral cortex development, we performed genome-wide mapping of E2A-bound sequences in primary NSCs using chromatin immunoprecipitation combined with DNA sequencing (ChIP-Seq). As splice variant-specific antibodies are not suitable for ChIP experiments due to their selective detection of DNA-bound regions, we used an antibody that recognizes both E12 and E47, and chromatin prepared from the mouse dorsal telencephalon at E12.5 (Fig. 3A), a stage when most cells in the cortex are progenitors and where E2A protein was highly abundant. Motif analysis of *cis*-regulatory sequences associated with E2A protein occupancy revealed that the E protein consensus DNA sequence (CAGCTG; E-box) was ranked as the top-scoring motif (Fig. 3B). E2A-bound regions were enriched for Sox family member and E2f6-binding motifs, suggesting coordinated DNA binding of E2A with these TFs (Fig. 3B). E2A-binding sites identified in this study compared with a previously published enhancer atlas of the developing cortex (Visel et al., 2013) and, together with H3K4Me1, H3K4Me3 and H3K27Ac histone marks (Shen et al., 2012), revealed that E2A predominantly bound enhancer regions (H3K27Ac, $H3K4Me1^{high}$, $H3K4Me3^{low}$), which are partially active as indicated by co-occurrence of p300. Promotor regions (H3K27Ac, $H3K4Me1^{low}$, $H3K4Me3^{high}$) that are bound by E2A in NSCs show p300 recruitment at later developmental stages (P0), indicating activity at later developmental time points (Fig. S4A). To determine the biological functions of E2A-bound genes according to enriched gene sets grouped by Gene Ontology (GO) terms, we used GREAT (Genomic Regions Enrichment of Annotations Tool). We found enrichment of the GO categories 'regulation of gliogenesis', 'brain development' and 'stem cell maintenance' (Fig. 3C). Several core genes responsible for the regulation of cortical brain development, including *Foxg1*, *Pax6* and *Sox5* are found within these enriched GO categories, suggesting that E2A serves as a central player in controlling corticogenesis. Currently, E2A target genes in embryonic NSCs during cortical development are unknown. Interestingly, although our ChIP-Seq did not reveal binding of E2A to previously described binding sites in the E-cadherin gene (Pérez-Moreno et al., 2001), we confirmed binding to sites in *Cdkn1a* [which encodes p21(CIP1) protein] (Fig. 3D) (Prabhu et al., 1997). Analysis of E2A occupancy of related CDKI genes in embryonic NSCs revealed several E2A-binding sites in the *Cdkn1b* [encodes p27(KIP1) protein] and *Cdkn1c* [encodes p57(KIP2) protein] loci (Fig. 3E,F). The three sites of E2A occupancy at the *Cdkn1c* locus in embryonic NSCs (Fig. 3F), which we termed 'p57-I' (intron), 'p57-II' (downstream) and 'p57-III' (distal intergenic) correspond to a potentially poised enhancer (H3K4Me1 only, p57-I), an active enhancer (H3K27Ac, H3K4Me1, p57-II) and a *Cdkn1c* promoter (H3K27Ac, H3K4Me3>H3K4Me, p57-III) (Fig. 3F), suggesting that these E2A-binding sites in the *Cdkn1c* locus are putative regulatory elements. Three biological replicates of the ChIP-Seq experiment showed a high degree of overlap between E2A-bound sites and, importantly, all E2A-binding sites within the *Cdkn1c* locus were confirmed (Fig. S4B).

E12 and E47 share binding sites with differential transcriptional outcome

To obtain genome-wide binding patterns of the E12 and E47 splice variant of E2A, we performed ChIP-Seq in $E12^{-/-}$ and $E47^{-/-}$ primary embryonic NSCs. Surprisingly, 67% of the identified E2A peaks were detected in both genotypes and greater than 90% of the reproducible E2A peaks in wild-type cells were also found by E2A in both E12- and E47-deficient primary embryonic NSCs (Fig. 4A). This indicates a high redundancy of E12 and E47 in their ability to recognize E2A enhancer. Motif analysis as well as GO enrichment for the overlapping E2A cistrome in these genotypes confirmed the results obtained in wild type (Fig. 3B,C), pointing out 'somatic stem cell maintenance', 'gliogenesis' and 'neurogenesis' among the most enriched pathways. Surprisingly, whole-genome transcriptome analysis by RNA sequencing (RNA-Seq) revealed astonishing differences in gene expression between $E12^{-/-}$ and $E47^{-/-}$ primary embryonic NSCs when compared with their respective littermate wild-type controls (Fig. 4B). Only 60 genes were identified as commonly differentially expressed in $E12^{-/-}$ and $E47^{-/-}$ cells (Table S1), emphasizing their distinct functions in this tissue. In order to identify the genes directly regulated by E12 and/or E47, we filtered the differentially expressed genes by the occurrence of a close by E2A peak in wild type (Venn diagram in Fig. 3B). 55.3% of the differentially expressed genes in $E47^{-/-}$ cells and 34.6% of the differentially expressed genes in $E12^{-/-}$ embryonic NSCs were predicted to be direct E2A target genes. A closer look at the direct E47 target genes (Table S2) revealed that 181 genes were induced upon loss of E47, whereas only 50 genes were repressed, indicating that E47 acts as a repressor in this context. In contrast, E12 target genes were mostly repressed (85 genes compared with 42 induced genes, Table S3), predicting an activating function of E12 at these loci. Besides the differences observed in the regulatory potential of

Development (2017) 144, 3917-3931 doi:10.1242/dev.145698

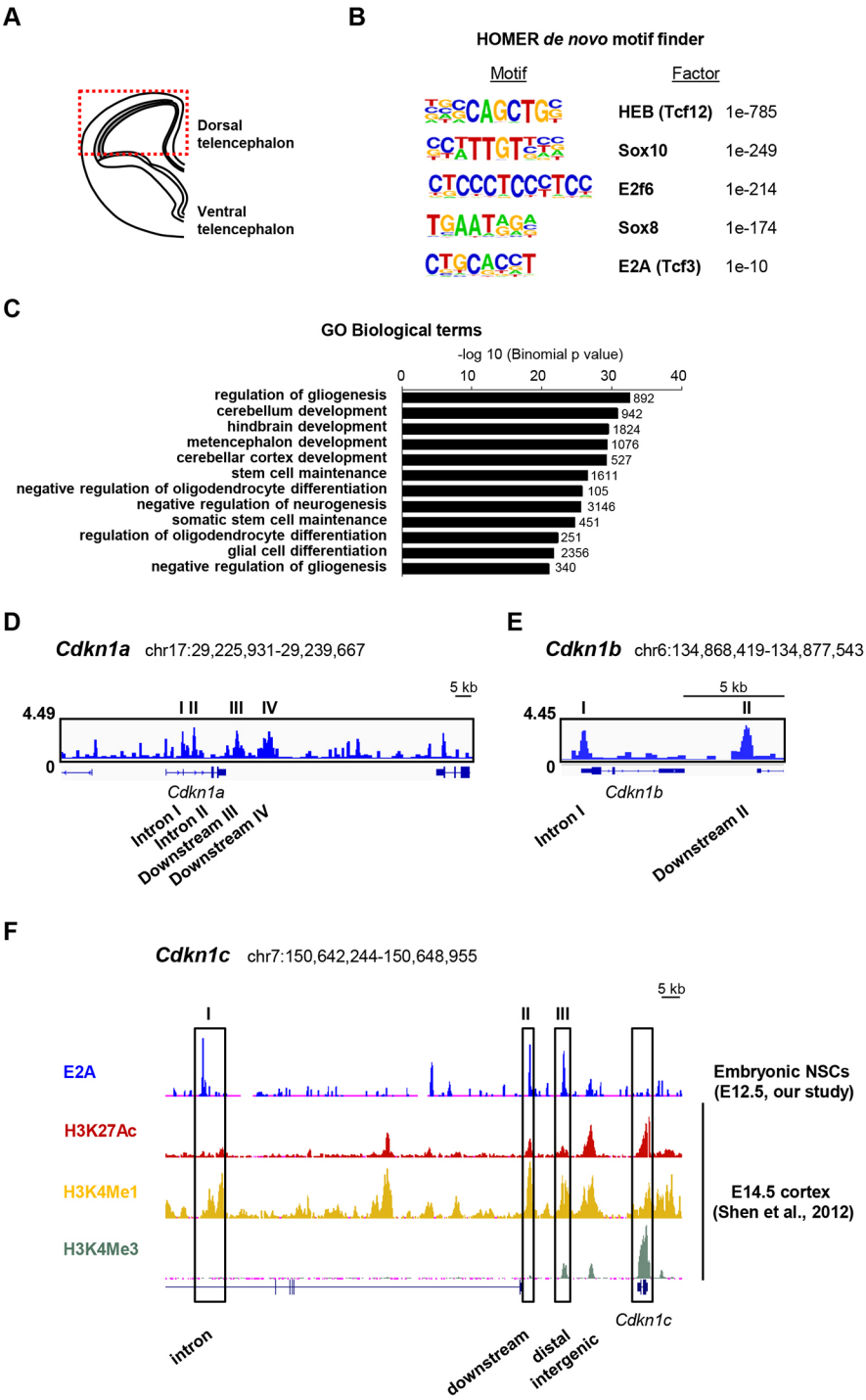

Fig. 3. Identification of E2A-binding sites in embryonic NSC chromatin using ChIP Seq. (A) Scheme of one cortical hemisphere at developmental stage E12.5. The red rectangle indicates the region of embryonic NSCs isolated for ChIP-Seq. (B) Motifs enriched in E2A-bound segments from a *de novo* search using HOMER software. *Cis*-regulatory sequences associated with E2A occupancy in embryonic NSCs were identified by comparison of enriched binding sites with randomly selected genomic DNA sequences. Letter size indicates nucleotide frequency. Log *P* values for the *cis*-regulatory sequences associated bHLH factor HEB (Tcf12), Sox10, E2f6, Sox8 and E2A (*Tcf3*) are indicated on the right. (C) Analysis of enrichment of Gene Ontology (GO) terms by GREAT for biological processes associated with E2A-bound genes. The number of target genes in each category is shown on the right of each bar. (D,E) A representative panel of E2A binding at the *Cdkn1a* locus (D) and *Cdkn1b* locus (E) in embryonic NSC chromatin. (F) A representative panel of E2A occupancy at the *Cdkn1c* locus in embryonic NSC chromatin in comparison with E2A histone marks in the cortex at E14.5 (Shen et al., 2012). Histone marks indicate that p57-I corresponds to a potential poised enhancer (H3K4Me1 only), whereas p57-II and p57-III are active enhancers (H3K27Ac, H3K4Me1). E2A peaks are indicated by roman numbers and peak heights are shown as numbers of sequenced reads.

the two E2A splice isoforms, GO enrichment analysis of the respective target genes revealed distinct functions for E47 and E12 in primary embryonic NSCs (Fig. 4B, right). E47 target genes induce biological processes as ‘negative regulation of glia cell differentiation’ (e.g. *Hmga2*, *Notch1*, *Dll3* and *Hes5*) and ‘negative regulation of nervous system development’ (e.g. *Ednrb* and *Lingo1*). E12 target genes on the other hand represent a variety of developmental biological processes (e.g. *Kit*, *Myc* and *Tgfbr2*), including ‘axon development’ (e.g. *Arhgef3* and *Nfasc*) and ‘cell-cell adhesion’ (*Sema4d* and *Has2*). To indicate the E2A binding pattern in wild-type, E12$^{-/-}$ and E47$^{-/-}$ embryonic NSCs of one of the genes differentially regulated by the E2A splice variants, we choose the *Cdkn1c* gene locus as an example (Fig. 3F, Fig. 4C). In wild-type NSCs, we observed four peaks upstream of the *Cdkn1c* gene locus (black boxes in Fig. 4C below wild-type track). These peaks are bound by E2A in E12$^{-/-}$ as well as in E47$^{-/-}$ embryonic NSCs. The strong signal in the E47$^{-/-}$ NSCs in intron 1 of the *Kcnq1* gene locus on the other hand was not identified as a peak by MACS and seems to be an artefact as many of the reads mapped here have identical start and end positions (PCR artefact, Fig. 4C). From analysis of E2A-binding events in wild-type, E12- and E47-deficient embryonic NSCs, we conclude that E12 and E47 are able

Development (2017) 144, 3917-3931 doi:10.1242/dev.145698

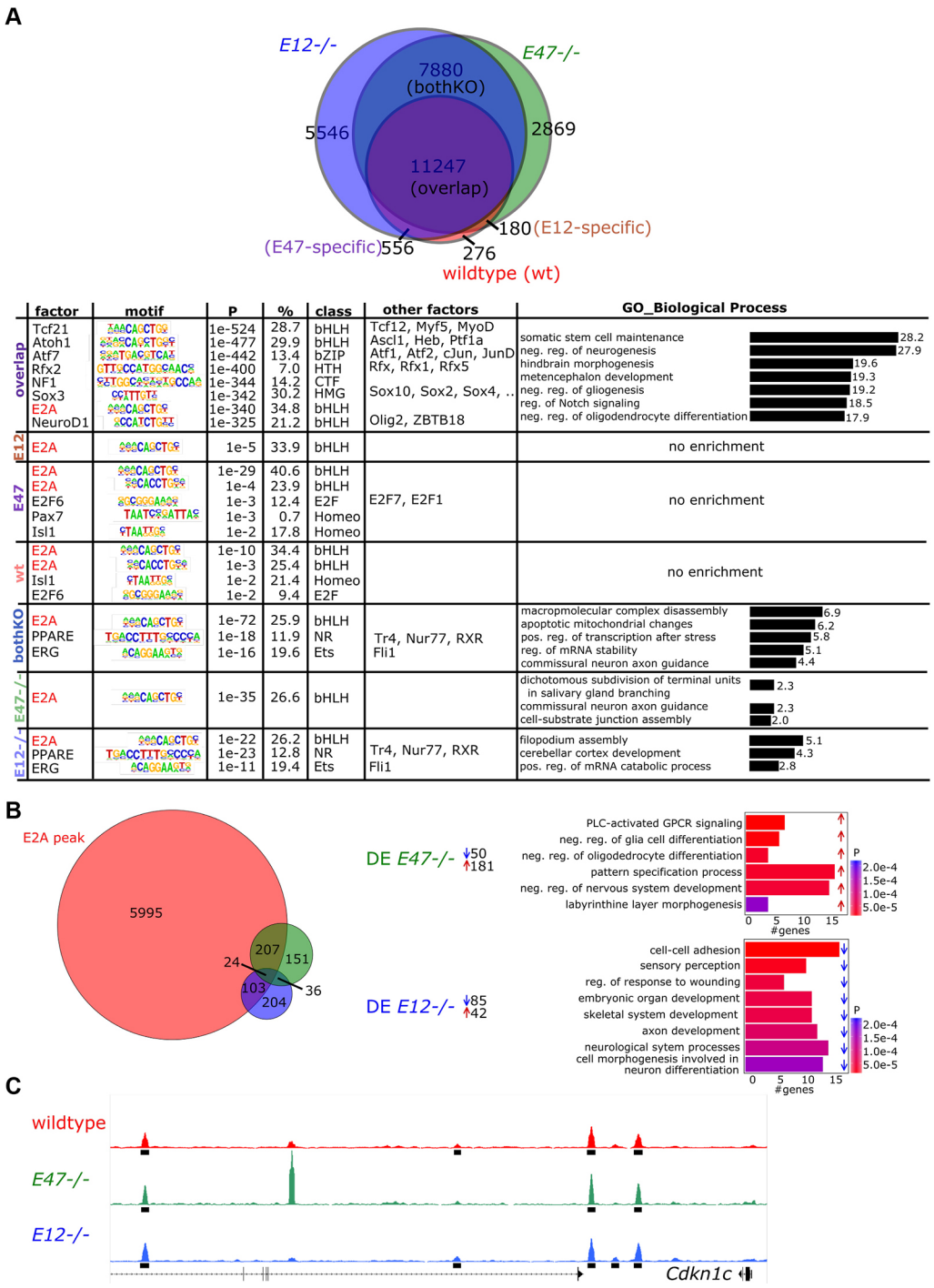

Fig. 4. Overlapping E47 and E12 cistromes with distinct transcriptional outputs. (A) ChIP-Seq analysis of E2A binding in wild-type, E12$^{-/-}$ and E47$^{-/-}$ primary embryonic NSCs. The Venn diagram indicates the proportion of E2A-binding sites overlapping or exclusively identified in wild-type, E12$^{-/-}$ and/or E47$^{-/-}$ NSCs, respectively. The table indicates the identified transcription factor-binding motifs and functional annotation according to the GO_Biological Process for each of the population subsets identified in the Venn diagram. The motifs identified from the overlapping E2A peaks of wild-type, E12$^{-/-}$ and E47$^{-/-}$ were also identified in all other E2A peak subsets and are not indicated repetitively. Overlap indicates common peaks in wild type, E12$^{-/-}$ and E47$^{-/-}$; both KO indicates shared E2A peaks in E12$^{-/-}$ and E47$^{-/-}$ but not wild-type peaks; E47$^{-/-}$indicates E2A peaks 'gained' in E47$^{-/-}$; E12$^{-/-}$ indicates E2A peaks 'gained' in E12$^{-/-}$; E47-specific indicates E2A peaks lost only in E47$^{-/-}$; E12-specific indicates E2A peaks lost only in E12$^{-/-}$. (B) Transcriptome analysis of E12$^{-/-}$ and E47$^{-/-}$ primary embryonic NSCs by RNA-Seq. The Venn diagram indicates the overlap in genes that are differentially expressed (fold change>1.5-fold) in E12$^{-/-}$ (blue) or E47$^{-/-}$ (green) cells compared with their respective wild-type littermate controls and the genes that have an E2A-binding site in their proximity. The bar plots indicate the functional annotation of the differentially expressed genes with a wild-type E2A peak close according to GO_Biological Process. Blue arrows refer to downregulation. Red arrows indicate upregulation. (C) UCSC tracks showing E2A binding in vicinity of the *Cdkn1c* locus in wild-type (red), E47$^{-/-}$ (green) and E12$^{-/-}$ (blue) NSCs. The black boxes indicate the peaks called by MACS2.

to bind the same sites, but differentially affect gene expression by recruitment of either differential interaction partners or co-regulators.

E47 directly regulates p57(KIP2) expression in embryonic NSCs by binding to a distal *Cdkn1c* enhancer

Next, we performed quantitative PCR using E47$^{-/-}$ embryonic NSCs to reveal whether E2A-bound CDKI genes were regulated by E47. Quantitative PCR revealed a halving, albeit not significant reduction of *Cdkn1c* mRNA expression in E47$^{-/-}$ embryonic NSCs compared with wild-type littermate cultures (Fig. S5A left), while *Cdkn1a* and *Cdkn1b* gene expression was not altered (Fig. S5A, middle, right). Immunolabeling for p57(KIP2) at E14.5 revealed a significant decrease in the p57(KIP2) expression in E47$^{-/-}$ embryos compared with wild-type embryos (Fig. 5A,B), while p57(KIP2) was not altered at E12.5 (Fig. S5B,C). In addition, no significant regulation of p57(KIP2) expression was observed in E12$^{-/-}$ embryos compared with wild-type embryos (Fig. S5D,E). To identify putative regulatory elements in the *Cdkn1c* locus that are controlled by E47, we cloned each of the identified E2A-binding regions (p57-I-III, Fig. 3F) upstream of a luciferase gene driven by the minimal *Admlp2* promoter and co-transfected HEK293T cells with these reporters and increasing amounts of E47. We found that E47 increased the activity of the 'p57-I' element in a dose-

Development (2017) 144, 3917-3931 doi:10.1242/dev.145698

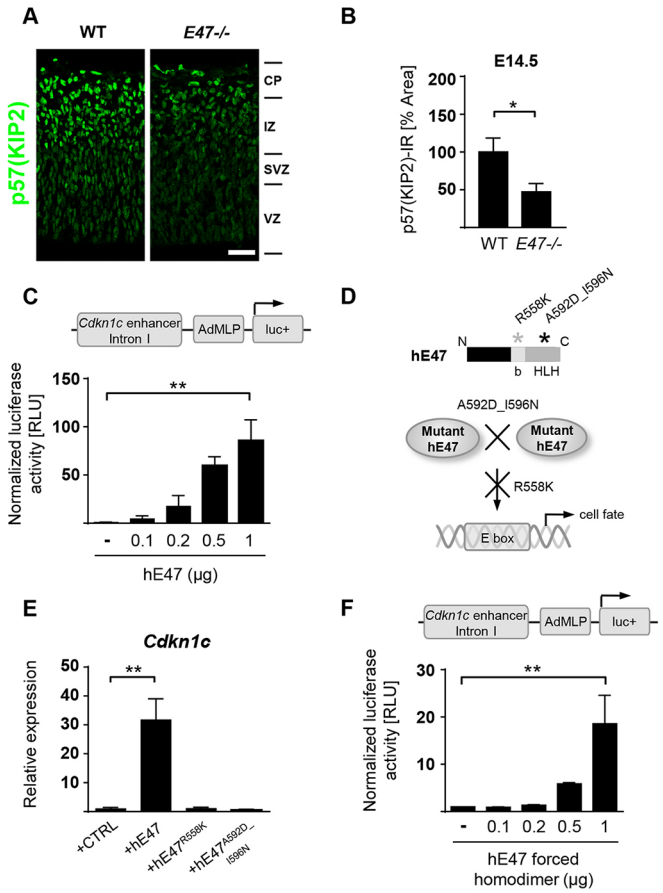

Fig. 5. E47 directly regulates p57(KIP2) expression in embryonic NSCs. (A) Immunolabeling for p57(KIP2) (A, green) in sagittal brain sections of E47$^{-/-}$ mice compared with wild-type littermates at E14.5. Scale bar: 40 µm. (B) Quantification of the p57(KIP2) immunoreactivity (n=6 wild-type mice, n=8 E47$^{-/-}$ mice). (C) Luciferase reporter assay in HEK293T cells using the indicated *Cdkn1c* luciferase reporter construct (*Cdkn1c* enhancer I termed as intron). Luciferase reporter assay results are of three independent experiments performed in duplicate. (D) Scheme illustrating mutations of the human E47 protein (mutation positions are indicated by asterisks). The hE47^{R558K}-IRES-eGFP plasmid encodes a hE47 mutant, which can dimerize and interact with potential co-factors, but cannot bind to the DNA. The hE47^{A592D_I596N}-IRES-eGFP plasmid encodes a hE47 mutant, which cannot dimerize with other bHLH TFs (Voronova and Baltimore, 1990). (E) Expression of *Cdkn1c* mRNA in embryonic NSCs 24 h after electroporation with the hE47 plasmid in comparison with cells electroporated with mutant hE47^{R558K}-IRES-eGFP and mutant hE47^{A592D_I596N}-IRES-eGFP plasmid or pCAGGs-IRES-eGFP control plasmid determined by quantitative PCR and normalized to *Gapdh*. Quantitative PCR results are of two independent experiments performed in duplicate. (F) Luciferase reporter assay in HEK293T cells using the indicated *Cdkn1c* luciferase reporter construct (*Cdkn1c* enhancer I termed as intron). Luciferase reporter assay results are from three independent experiments performed in duplicate. Data are mean±s.e.m. **P<0.01; *P<0.05 by Student's t-test (B) and one-way ANOVA (C,E,F). RLU, relative light unit.

dependent manner [human E47 (hE47), 86±21.59-fold (±s.e.m.), P<0.01; Fig. 5C], whereas E47 did not significantly affect the activities of the 'p57-II' and 'p57-III' regions (Fig. S5F,G). We next analyzed whether dimerization and DNA binding of E47 is required for *Cdkn1c* expression. Therefore, we used either an E47 mutant that cannot form homo- or heterodimers (A592D_I596N) owing to mutations in the HLH region (black asterisk) or an E47 mutant that is able to form dimers but cannot bind DNA (R558K) due to a mutation in the basic region of the protein (gray asterisk) (Fig. 5D) (Voronova and Baltimore, 1990). Equal expression of the E47 mutants in embryonic NSCs was validated by western blot analysis (Fig. S5H). *Cdkn1c* mRNA expression was significantly increased in cells expressing wild-type hE47 in comparison with control cell cultures electroporated with an empty vector [hE47, 33±7.26-fold (±s.e.m.); P<0.01; Fig. 5E]. In accordance with the mRNA expression data of *Cdkn1a* and *Cdkn1b* in E47$^{-/-}$ embryonic NSCs (Fig. S5A, middle, right), hE47 expression in embryonic NSCs did not alter *Cdkn1a* and *Cdkn1b* gene expression (Fig. S5K). To test whether E47 interacts with proneural bHLH factors to regulate *Cdkn1c*, we performed co-immunoprecipitation on lysates from embryonic neural stem cells. E47 did not interact with any tested non-bHLH proteins (Limk) nor with bHLH TFs (NeuroD1, NeuroD2, Math2, Mash1, and Ngn2) in primary NSCs, suggesting a yet unknown interaction partner for E47 or E47 might primarily act as a homodimer (Fig. S5I). Indeed, overexpression of an E47 forced homodimer (E47FD) (Sigvardsson et al., 1997) (Fig. S5J, validation of expression by western blot analysis) increased the activity of the 'p57-I' element in a dose-dependent manner (Fig. 5F).

E47 overexpression regulates NSC differentiation and localization

The E47 regulated CDKI p57(KIP2) has been shown to regulate cellular processes, including proliferation, cell cycle exit and differentiation of embryonic NSCs (Mairet-Coello et al., 2012; Tury et al., 2011, 2012). To determine the role of E47 in these biological processes, we analyzed cortices of E47$^{-/-}$ embryos and control littermates for cell proliferation (Ki67^{+} cells) and for cell cycle dynamics by analyzing cumulative EdU labeling (2-h intervals) in Ki67^{+} neuronal precursors. We did not detect any significant differences in cell proliferation and cell cycle length in E47$^{-/-}$ embryos at E14.5 compared with control littermates (Fig. 6A,B) or at E12.5 (Ki67^{+} neuronal cell and Edu^{+}Ki67^{+} cells at 2 h after injection, data not shown). In addition, immunostaining for phosphohistone H3 (pH3), an indicator of late G2- and M-phase (Hendzel et al., 1997) revealed no difference in apical and basal divisions in E47$^{-/-}$ embryos at E14.5 compared with control littermates (Fig. 6C,D and data not shown). Accordingly, neither proliferation nor apoptosis of E47$^{-/-}$ embryonic NSCs was altered compared with wild-type cells *in vitro* (Fig. 6E,F; Fig. S6A,B). However, analysis of E47$^{-/-}$ embryonic NSCs revealed a difference in the distribution of the size of neurospheres formed compared with wild-type embryonic NSCs, with increased numbers of bigger neurospheres formed by E47$^{-/-}$ compared with wild-type cells (Fig. S6C). Yet, the total number of single cells within the dissociated neurospheres did not differ between E47$^{-/-}$ and control cells (data not shown), suggesting no difference in proliferation, but possibly differences in single cell size or cell-adhesion properties (Marthiens et al., 2010). To identify whether E47 regulates NSC differentiation, we overexpressed E47 in primary embryonic NSCs, which resulted in a reduced number of cells with neurite outgrowth [hE47, 23.1±6.3% and control, 75.48±6.8% (±s.e.m.); P<0.01: Fig. 7A,B] compared with control NSCs (pCAGGs-IRES-eGFP, referred to as CTRL). Furthermore, overexpression of the E47 non-DNA-binding mutant (hE47^{R558K}) showed an increased number of cells with neurite outgrowth compared with wild-type hE47 overexpression (Fig. 7A,B). We next investigated the effect of E47 on neuronal differentiation and localization *in vivo* by *in utero* electroporation of wild-type embryos at E13.5. E47-overexpressing cells (GFP^{+}) showed reduced neurite outgrowth [hE47, 7.45±4.0% and control, 50.22±4.78% (±s.e.m.); P<0.001: Fig. 7C,D] and had a

Development (2017) 144, 3917-3931 doi:10.1242/dev.145698

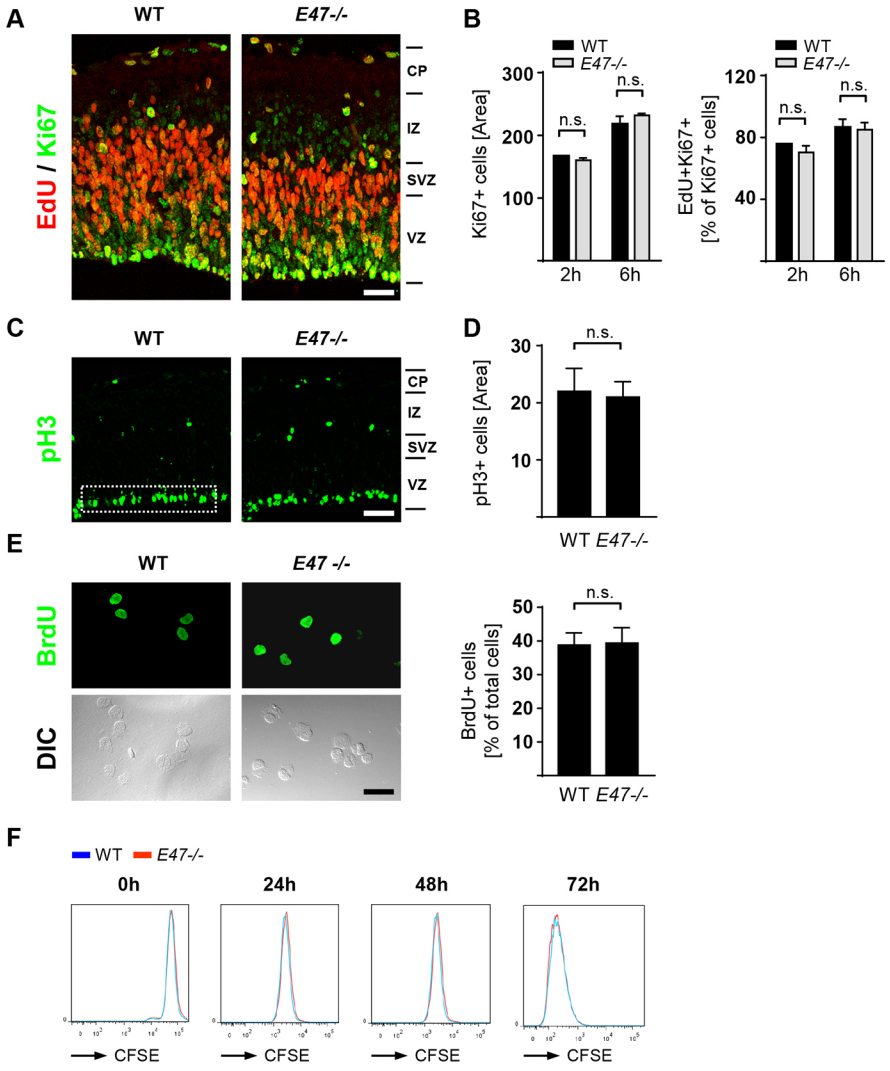

Fig. 6. E47 deficiency does not affect cell cycle length of embryonic NSCs and intermediate precursor cells. (A) Immunolabeling for EdU (red) in combination with Ki67 (green) in the cortex in sagittal brain sections of E47$^{-/-}$ mice and wild-type littermates at E14.5 2 h after EdU injection. Scale bar: 40 µm. (B) Quantification of the number of proliferating precursors (Ki67^{+}) (*n*=3 wild-type mice, *n*=4 E47$^{-/-}$ mice) and quantification of the number of proliferating precursors and SVZ precursors in S phase (Ki67^{+}EdU^{+} per Ki67^{+}) per area of quantification (*n*=1 wild-type mice, *n*=3 E47$^{-/-}$ mice, 2 h; *n*=2 wild-type mice, *n*=2 E47$^{-/-}$ mice, 6 h). (C) Immunolabeling for phospho-histone H3 (green) in sagittal brain sections of E47$^{-/-}$ mice and wild-type littermates at E14.5. Scale bar: 55 µm. (D) Quantification of the number of phospho-histone H3^{+} cells (*n*=5 wild-type mice, *n*=4 E47$^{-/-}$ mice). (E) Immunolabeling for BrdU of E47$^{-/-}$ and wild-type embryonic NSCs after a 4 h BrdU pulse (left) and quantification of immunolabeled BrdU^{+} cells (right). Scale bar: 20 µm. BrdU labeling results are from four independent experiments. A minimum of 200 cells per condition were analyzed. (F) Labeling of E47$^{-/-}$ and wild-type embryonic NSCs by CFSE and measurement of CFSE intensity by flow cytometry 0, 24, 48 and 72 h after labeling. CFSE labeling results are from two independent experiments. Data are mean±s.e.m. *P*-values were calculated using Student's *t*-test. BrdU, 5-bromo-2′-deoxyuridine; CFSE, carboxyfluorescein succinimidyl ester; DIC, differential interference contrast; EdU, 5-ethynyl-2′-deoxyuridine; CP, cortical plate; IZ, intermediate zone; SVZ, subventricular zone; VZ, ventricular zone; pH3, phospho-histone H3.

more apical position in the cortex, mainly in the IZ [hE47, 0.22±0.22, and control, 1.00±0.14 (±s.e.m.); $P<0.05$: Fig. 7C,E]. E47 overexpressing cells did not differentiate into Tbr1^{+} deep layer neurons, as did controls (Fig. 7F). Further characterization of the E47 overexpression cells revealed that these cells are NeuroD1^{+} intermediate zone precursor cells (Fig. 7G, Fig. S7). The E47-regulated CDKI p57(KIP2) has been shown to regulate cellular processes, including differentiation of embryonic NSCs (Mairet-Coello et al., 2012; Tury et al., 2011, 2012). To investigate, whether E47 regulates NSC differentiation via regulation of p57(KIP2), we overexpressed p57(KIP2) in primary embryonic E47$^{-/-}$ NSCs. E47$^{-/-}$ NSCs already had a tendency to have an increased number of cells with neurite outgrowth when compared with wild-type NSCs (Fig. 7H,I). Importantly, p57(KIP2) overexpression in primary embryonic E47$^{-/-}$ NSCs resulted in a reduced number of cells with neurite outgrowth {mouse p57(KIP2) [mp57 (KIP2)], 23.5±9.5%; control, 43.7±10.4% (±s.e.m.); $P<0.01$: Fig. 7H,I}. In line with these results, *in vivo* overexpression of E47 resulted in increased p57(KIP2) expression, while p57 (KIP2) protein could not be detected in sections of embryos electroporated with control plasmid (Fig. 7J,K). Together, these results suggest that, in embryonic NSCs, increased abundance of E47 leads to impaired neuronal differentiation and localization by upregulation of the CDKI p57(KIP2).

DISCUSSION

The *Tcf3* locus (E2A) encodes two highly related proteins, E12 and E47, that arise through mutually exclusive splicing of two alternative exons and differ only in their DNA-binding region (Murre et al., 1989). Recently, distinct roles for E12 and E47 in B cell specification have been demonstrated (Beck et al., 2009). Our results suggest that the E2A splice variant E47 is required for proper neuronal differentiation and layer-specific localization, whereas the E2A splice variant E12 is likely dispensable for early corticogenesis. E2A regulates cell type specification and differentiation programs, including neurogenesis during embryonic development, by dimerization with tissue-specific class II HLH proteins (Gradwohl et al., 1996; Lee, 1997; Wang and Baker, 2015). Thus, an important unresolved issue is whether E2A functions independently of neurogenic class II bHLH TFs. *Ngn2;Mash1* double-mutant embryos have a severe disruption of the cortical cytoarchitecture (Nieto et al., 2001) and *Ngn* mutant embryos show a specification defect of neural precursor cells, resulting in abnormal localization of early-born deep-layer neurons during dorsal telencephalon development (Casarosa et al., 1999; Fode et al., 2000; Li et al., 2012; Nieto et al., 2001; Schuurmans et al., 2004). In contrast, our data revealed a specific role for E47 in regulating the population size of Tbr1^{+} and Satb2^{+} projection neurons, while neuronal regional identity and the overall cortical

Development (2017) 144, 3917-3931 doi:10.1242/dev.145698

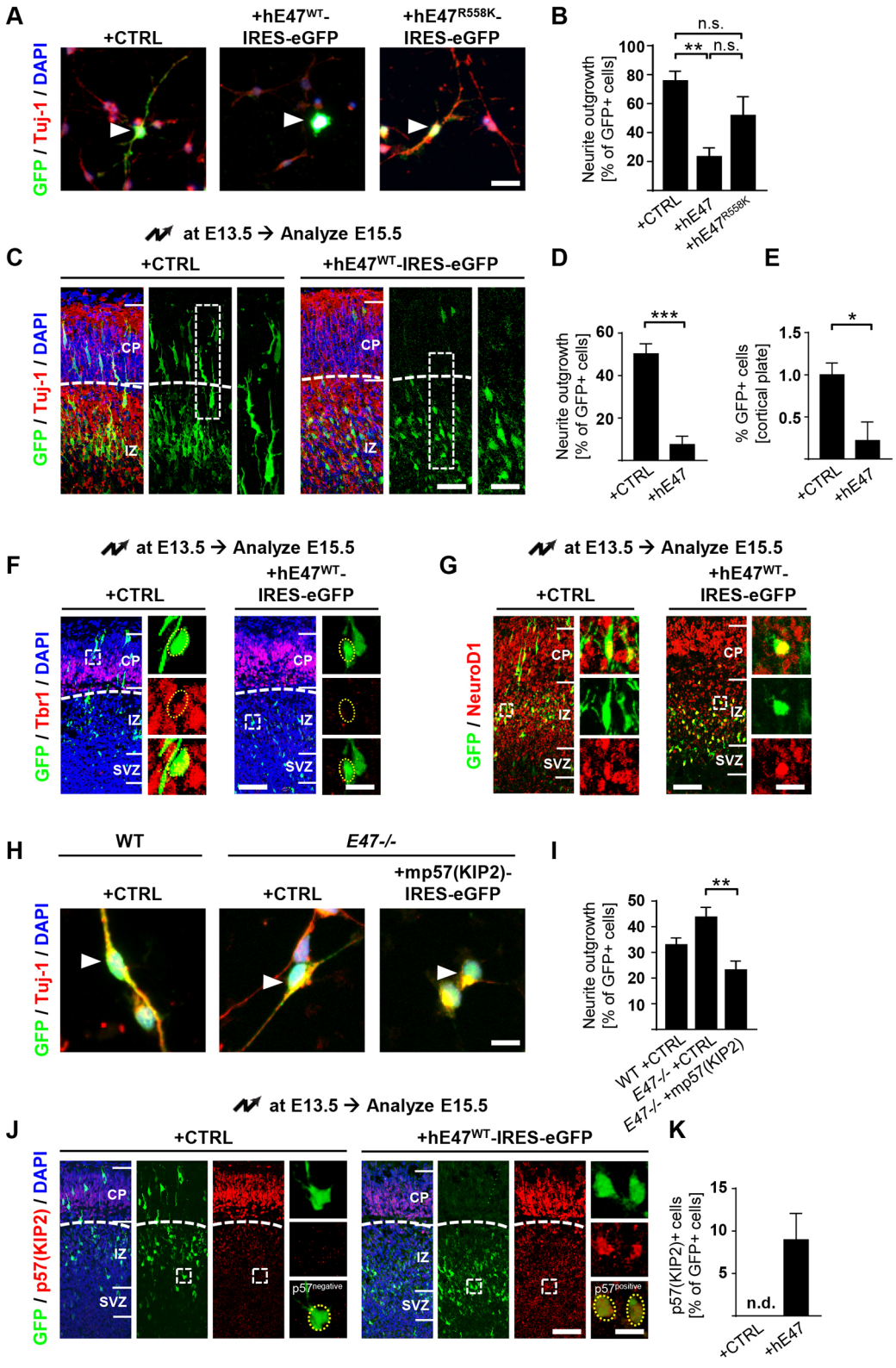

Fig. 7. See next page for legend.

cytoarchitecture was not affected. Thus, with regard to heterodimerization with class II bHLH TFs, Mash1 and Ngn are not strictly dependent on E47. The interaction with Mash1 as a key TF in ventral telencephalon development is unlikely to mediate E47-regulated differentiation of projection neurons with dorsal telencephalon identity (Fode et al., 2000), as it was shown that the specification of these cells is Ngn dependent. Furthermore, E47 might function independently of Ngn during early neurogenesis, as Ngn1/Ngn2 are required to specify the cortical, glutamatergic and laminar characteristics of early-born neurons, while simultaneously

Development (2017) 144, 3917-3931 doi:10.1242/dev.145698

Fig. 7. E47 regulates NSC differentiation via p57(KIP2). (A) Immunolabeling for Tuj-1 (red, neurons) and GFP (green, electroporated cells) 2 days after electroporation of primary NSCs with wild-type hE47 plasmid (hE47^{WT}-IRES-eGFP) in comparison with mutant (hE47^{R558K}-IRES-eGFP) and control plasmid (CTRL, pCAGGs-IRES-eGFP) cultured under differentiation conditions on laminin. Nuclei are stained with DAPI (blue). Arrowhead indicates a representative electroporated cell per condition. Scale bar: 20 µm. (B) Quantification of the number of electroporated GFP$^+$ cells showing neurite outgrowth in embryonic NSCs overexpressing wild-type hE47, hE47^{R558K} or control plasmid. Results are from four different experiments. A minimum of 130 cells per condition was analyzed. (C) *In utero* electroporation of wild-type mice at E13.5 with either pCAGGs-IRES-eGFP or hE47^{WT}-IRES-eGFP. Immunolabeling was performed for Tuj-1 (red, neurons) and GFP (green, electroporated cells) in sagittal brain sections at E15.5. Enlargements of regions outlined show inhibition of neurite outgrowth and mislocalization of cells expressing hE47^{WT}-IRES-eGFP (right) compared with control (pCAGGs-IRES-eGFP) (left). Nuclei are stained with DAPI (blue). Scale bars: 40 µm (left); 20 µm (right). (D,E) Quantification of the number of GFP$^+$ cells showing neurite outgrowth (D) or located in the cortical plate (CP) (E) in sections of E15.5 embryos after *in utero* electroporation (D: *n*=3 CTRL, *n*=4 hE47; E: *n*=6 CTRL, *n*=5 hE47). (F,G) Immunolabeling for Tbr1 (F, red, deep layer neurons), NeuroD1 (G, red, intermediate zone cells) and GFP (green, electroporated cells) in sagittal brain sections at E15.5. Enlargements of regions outlined show E47-overexpressing cells that are GFP$^+$Tbr1$^-$ cells (right) compared with control cells that are GFP$^+$Tbr1$^+$ cells (left) (F), and NeuroD1$^+$GFP$^+$ cells in the intermediate zone (G). Nuclei are stained with DAPI (blue).
(H) Immunolabeling for Tuj-1 (red, neurons) and GFP (green, electroporated cells) 1 day after electroporation of primary E47$^{-/-}$ NSCs with mp57(KIP2) plasmid [mp57(KIP2)-IRES-eGFP] in comparison with control plasmid (pCAGGs-IRES-eGFP) cultured under differentiation conditions on laminin. Nuclei are stained with DAPI (blue). Arrowheads depict a representative electroporated cell per condition. Scale bar: 10 µm. (I) Quantification of the number of electroporated GFP$^+$ cells showing neurite outgrowth in embryonic E47$^{-/-}$ NSCs overexpressing mp57(KIP2) or control plasmid. Results are from four different experiments. A minimum of 100 cells per condition was analyzed. (J) *In utero* electroporation of wild-type mice at E13.5 with either pCAGGs-IRES-eGFP or hE47^{WT}-IRES-eGFP. Immunolabeling for p57(KIP2) (red) and GFP (green) was performed in sagittal sections of the cortex at E15.5. Enlargements of regions indicated by rectangles show GFP$^+$p57(KIP2)$^+$ cells (right, yellow circle) and GFP$^+$p57(KIP2)$^-$ cells (left, yellow circle). Scale bars: 65 µm (left); 10 µm (right). Nuclei are stained with DAPI (blue).
(K) Quantification of the number of p57(KIP2)$^+$GFP$^+$ cells in sections of E15.5 embryos after *in utero* electroporation (*n*=3 pCAGGs-IRES-eGFP, *n*=4 hE47-IRES-eGFP). Data are mean±s.e.m. ***P<0.001; **P<0.01; *P<0.05 using one-way ANOVA (B,I) and Student's *t*-test (D,E,K). Dotted line indicates the border between the cortical plate (CP) and IZ/SVZ area (C,F,G,J). CP, cortical plate; IZ, intermediate zone; SVZ, subventricular zone.

repressing an alternative subcortical, GABAergic neuronal phenotype (Schuurmans et al., 2004). In contrast, E47 regulated the differentiation of Tbr1-positive deep layer and Satb2-positive upper layer projection neurons at E14.5, whereas E47 depletion did not result in an alternative subcortical, GABAergic neuronal phenotype. At this point a role for E2A as a heterodimerization partner of neurogenic class II bHLH TFs during early dorsal telencephalon development cannot be excluded; in E47-deficient embryos, other E proteins, such as E12, E2-2 and HEB might compensate for the loss of E47 at specific developmental time points. Our data revealed overlapping expression of E47 and E12 in NSCs and our ChIP-Seq identified a big overlap for E12- and E47-specific binding sites in embryonic NSCs, supporting possible functional redundancy among individual E proteins at different developmental time points. However, protein stability in differentiating cells (Fig. 1G), post-translational modifications (Teachenor et al., 2012), heterodimerization partner or co-factor recruitment (Gow et al., 2014) at specific developmental time points in specific cell populations further adds complexity to the specific functions of individual E proteins in cortical development. Indeed, our RNA-Seq analysis revealed that the splice-isoform E47 acts mainly as a transcriptional repressor in NSCs, while E12 target genes are reduced in E12$^{-/-}$ primary embryonic NSCs, pointing towards a distinct transcriptional regulatory mechanism exploited by each of the two E2A splice isoforms.

As E47 overexpression *in vitro* and *in vivo* showed neuronal differentiation defects resulting in impaired neurite outgrowth, another potential interaction partner could be NeuroD due to its function in neuritogenesis (Bayam et al., 2015; Ince-Dunn et al., 2006). Indeed, the comparison of our E2A ChIP-Seq data with a genome-wide NeuroD2 DNA-binding analysis (Bayam et al., 2015) revealed largely overlapping NeuroD2 binding around E2A peaks, including the 'p57-I' intronic enhancer of *Cdkn1c*. We detected no interaction of E47 with putative binding partners, including NeuroD1/2 in primary embryonic NSCs, suggesting a potential role for E47 homodimers. Indeed, our luciferase assays revealed that E47 homodimers regulate *Cdkn1c* expression independently of pro-neurogenic class II bHLH heterodimerization partner. Future studies will show whether E47 might act as a homodimer or in combination with an as yet unknown TF to regulate the differentiation of Tbr1$^+$ and Satb2$^+$ projection neurons.

E2A proteins play key roles in controlling gene expression during development of many tissues, such as in B and T cell development (Murre, 2005). Yet, no E2A target genes are known for cortex development. Target genes have been described for the potential E2A interaction partners Mash1, Ngn1/2 and NeuroD. A genome-wide study for Mash1 characterized target genes during ventral telencephalon development (Castro et al., 2011), whereas a genome-wide study for NeuroD2 (genes with functions in layer-specific differentiation and in axonal pathfinding) and target genes for Ngn2 [*Etv1*, *HuD* (*Elav4*) and *Rnd2*] have been described for dorsal telencephalon development (Bayam et al., 2015; Bronicki et al., 2012; Heng et al., 2008; Kovach et al., 2013). The E2A-activated transcriptional program described here provides evidence that E2A indeed induces many TFs and other regulators of specification and differentiation of embryonic NSCs, e.g. Foxg1 (Martynoga et al., 2005), Pax6 (Warren et al., 1999) and Sox5 (Kwan et al., 2008), suggesting that E2A is actively involved in the balanced coordination of the neurogenic program in cortical development.

E proteins are not functionally equivalent as they function independently, resulting in E protein-specific phenotypes (Beck et al., 2009) and as they regulate specific target genes in different immune cell lineages (Lin et al., 2010; Sanda et al., 2012); however, no E2A splice variant target genes are known for cortex development. Our genome-wide DNA-binding analysis of E12 and E47 revealed similar binding patterns of both splice variants. E2A peaks 'lost' in splice variant-deficient mice suggest occupancy of E47 and E12 splice variant homo- or heterodimerzation at E2A binding sites. We speculate at this point that the two splice variants of E2A are able to compensate for each other's loss at the level of target site DNA binding. In contrast, RNA-Seq analysis of target gene regulation revealed a unique role for E12 and E47 in regulating transcription of certain genes. Specifically, our data suggest that E47 might mainly work by repressing genes, while E12 seems to work as a transcriptional activator of genes in embryonic neural stem cells. This is in line with a role for E47 as a transcriptional repressor of a subset of astrocyte-specific genes in adult NSC differentiation (Bohrer et al., 2015). E2A binding to the *Cdkn1c* gene locus was detected in E12- and E47-deficient embryonic NSCs, albeit expression of *Cdkn1c* was altered only upon deletion of E47 and remained stable in the absence of E12. Thus, splice

Development (2017) 144, 3917-3931 doi:10.1242/dev.145698

variant-specific transcriptional gene regulation detected in our study were in line with phenotypic differences observed in E12$^{-/-}$ and E47$^{-/-}$ mice, suggesting that E12 and E47 might have similar DNA-binding capabilities, but splice-variant specific DNA binding may result in distinct regulatory mechanisms (e.g. by recruitment of different co-regulators) that differentially affect gene expression. This may affect gene expression of various other genes and not only of *Cdkn1c* during cortical development.

A function for E2A as cell cycle regulator has been proposed and E2A-binding sites in CDKI genes have been described outside the nervous system (Pagliuca et al., 2000; Prabhu et al., 1997). Although our study identified E2A-binding sites in the *Cdkn1a*, *Cdkn1b* and *Cdkn1c* loci, E47 overexpression, knockout experiments and luciferase reporter assays revealed that, among those, only the *Cdkn1c* gene is a regulated E47 target gene during cortical development. A previous study indicated that potential *Cdkn1c* enhancers are located between +35 and +225 kb from the *Cdkn1c* transcription start site (John et al., 2001) and a putative muscle-specific enhancer was recently identified to be localized to a conserved 686 bp fragment lying ∼+59 kb from *Cdkn1c* that is controlled by the bHLH TF MyoD (Zalc et al., 2014). This muscle-specific enhancer element corresponds to one site of E12 and E47 occupancy in embryonic NSCs ['p57-I' (intron)] identified by our ChIP-Seq data and was classified as a poised enhancer in mESCs by analyzing histone marks (Shen et al., 2012). Furthermore, E47 was able to activate transcription from this enhancer, suggesting that it not only acts as an enhancer in muscle cell differentiation, but might be developmentally regulated in several tissues. However, here it is not activated by MyoD, but presumably by E47 heterodimers or homodimers, and functions as a regulatory element in neuronal localization and differentiation during corticogenesis.

Cell cycle and differentiation in the developing forebrain are intimately connected (Salomoni and Calegari, 2010; Tury et al., 2011). Blocking the cell cycle induces neural-progenitor differentiation and migration from the VZ to upper cortical regions (Calegari and Huttner, 2003; Lange et al., 2009). p57 (KIP2) as a member of CDKIs is able to block the progression of the cell cycle in embryonic (Furutachi et al., 2015) and adult NSCs (Furutachi et al., 2013) by predominantly binding and inhibiting cyclin/CDK complexes of the G1 phase. Surprisingly, we did not observe functions of E47 for the regulation of cell proliferation and cell cycle length during early cortical development at E14.5. In addition to the well-characterized function of p57(KIP2) in regulating cell cycle progression, it also has been shown to control NSC migration and differentiation (Mairet-Coello et al., 2012; Tury et al., 2011, 2012). *Cdkn1c*-deficient mice reveal an increase in layer V to VI neurons (Mairet-Coello et al., 2012). Despite E2A and p57(KIP2) expression in SVZ/IZ cells during early- and mid-corticogenesis (Fig. 1C, Fig. S1C) (Tury et al., 2012; data not shown), E47 might regulate p57(KIP2) expression in a defined time window to control Tbr1$^+$ and Satb2$^+$ cortical projection neuron differentiation at mid-neurogenesis. Indeed, our data revealed that E47 regulated p57(KIP2) at a specific developmental time point during corticogenesis.

Interestingly, p57(KIP2) regulates cell differentiation and migration via direct interaction with several bHLH TFs, such as Mash1, NeuroD1/2 and Nex/Math2, and actin cytoskeleton-modifying enzymes, such as Limk1/2 (Joseph et al., 2009; Vlachos and Joseph, 2009). NeuroD2 was recently identified as an early-onset neuronal transcript with protein expression detected in newborn apical VZ neurons (Telley et al., 2016) and p57(KIP2) expression was shown to colocalize with NeuroD1 in postmitotic cells in the IZ (Tury et al., 2012). Our data showed that the overexpression of p57(KIP2) in E47$^{-/-}$ NSCs inhibited neurite outgrowth, similar to E47 overexpression in wild-type NSCs, suggesting a linear relationship between E47 and p57(KIP2) expression in the differentiating projection neurons during cortical development. Future studies will determine whether E47 dynamically controls p57(KIP2) expression, which then might direct neurogenesis of Tbr1$^+$ and Satb2$^+$ projection neurons by abundant p57(KIP2) interacting with NeuroD.

We identified a specific role for E47 in regulating Tbr1$^+$ and Satb2$^+$ projection neurons via p57(KIP2) during cortical development, while Ctip2$^+$ projection neurons were not affected. The sequence and pace of neuronal differentiation processes of different neuronal subtypes is instructed by sequential transcriptional waves (Telley et al., 2016). The birthdates of cortical neurons are known to correspond to their particular cortical layer position (Smart and Smart, 1982), as is the case for layer VI Tbr1$^+$ and layer V Ctip2$^+$ subcortical layer projection neurons. Birthdating experiments revealed that even Ctip2$^+$ neurons in layer V are earlier born than Satb2$^+$ callosal projection neurons in layer V (Hatanaka et al., 2016). Therefore, E47 might control distinct temporally gated genetic targets and networks in different cell populations, such as the identified p57(KIP2) target in this study, that affect distinct neuronal subpopulation localization and differentiation. Misbalanced neurogenesis is associated with autism-like features (Fang et al., 2014) and, more specifically, altered Tbr1 expression and function is associated with autism (Deriziotis et al., 2014; Huang et al., 2014; Notwell et al., 2016). As E47 is regulating Tbr1$^+$ and Satb2$^+$ projection neuron cell numbers during cortical development, it would be very interesting to investigate whether dysregulated E47 is linked to Tbr1-related autism spectrum disorders.

Overall, we identified a specific role for E47 in regulating Tbr1$^+$ and Satb2$^+$ projection neurons via p57(KIP2) during cortical development. Beside its function in brain development, p57(KIP2) has been implicated in adult NSC quiescence and neurogenesis (Furutachi et al., 2013, 2015), cancer (Borriello et al., 2011; Guo et al., 2010), and human disorders (Duquesnes et al., 2016; John et al., 2001; Zhang et al., 1997). The *Cdkn1c* locus has been implicated in the Beckwith-Wiedemann syndrome, a growth-regulation disorder characterized by tissue overgrowth and predisposition to tumors (Zhang et al., 1997), and mutations in different predicted enhancers have been suggested to contribute to the formation of the disease (Eggermann et al., 2014). Aberrant p57 (KIP2) expression might be evoked through misbalanced E47 protein activity or mutations in the E47-responsive enhancer. Thus, the consequent targeting of E47 activity and the direct regulation of p57(KIP2) by the distant E47-regulated 'p57-I' enhancer identified in this study might offer novel therapeutic opportunities for p57 (KIP2)-associated diseases.

MATERIALS AND METHODS

Animals

C57BL/6J mice (Jackson Laboratory), C57BL/6J-inbred mice deficient for the E2A splice variant E12 (E12$^{-/-}$) or E47 (E47$^{-/-}$) (Beck et al., 2009), *Eomes*^{GFP} mice (Arnold et al., 2009) and *Hes5::CreE*^{RT}*2Rosa26-CAG::eGFP*$^{fl/+}$ (Rolando et al., 2016) were used. Mouse brains were isolated from embryos of various developmental stages as indicated. The morning of vaginal plug was considered as being embryonic day 0.5 (E0.5). All animal experiments were approved by the Federal Ministry for Nature, Environment and Consumer Protection of the state of Baden-Württemberg and were performed in accordance to the respective national, federal and institutional regulations.

Development (2017) 144, 3917-3931 doi:10.1242/dev.145698

Immunohistochemistry

Embryonic mouse brains were dissected and fixed in 4% paraformaldehyde (PFA) in phosphate-buffered saline (PBS) at 4°C overnight. After cryoprotection by immersion in 30% sucrose solution, brain samples were embedded in OCT (Tissue-Tek). Immunohistochemistry on sagittal brain cryostat sections was performed as described previously (Schachtrup et al., 2015). Details of immunohistochemistry and antibodies used are described in the supplementary Materials and Methods.

In situ hybridization (ISH)

Nonradioactive ISH was performed on cryosections of wild-type mice using a *Tcf3*-specific probe. For details of ISH, see the supplementary Materials and Methods.

Embryonic NSC culture

Embryonic NSCs from E14.5 embryos were isolated and cultured as described (Bohrer et al., 2015; Reynolds and Weiss, 1992). For differentiation conditions, embryonic NSCs were plated on laminin (1 µg/ml; Sigma-Aldrich) in NSC medium without rhFGF-2 and rhEGF. For neurosphere size measurements, 200 dissociated embryonic NSCs per well were cultured in a 96-well plate (BD) in NSC medium with growth factors for 7 days. The diameter of at least 200 neurospheres was measured as recently described (Nam and Benezra, 2009). For proliferation assays, dissociated embryonic NSCs were cultured in NSC proliferation medium for 24 h, treated with BrdU (1:100, Invitrogen) for 4 h, followed by cytospin and immunolabeling. Additionally, proliferation was tested by labeling NSCs with carboxyfluorescein diacetate succinimidyl ester (CFSE) by incubating 2×10^6 cells/ml in PBS containing 1 µM CFSE for 10 min at 37°C. Embryonic NSCs were harvested at different time points, resuspended in FACS buffer (PBS+1% BSA) containing propidium iodide (1 µM), and immediately analyzed by flow cytometry. Data were collected with the LSRII flow cytometer (BD Biosciences) and analyzed with FlowJo software (Tree Star). For E47 overexpression experiments, wild-type embryonic NSCs were transfected by electroporation using the Mouse Neural Stem Cell Nucleofector Kit (Lonza) following the manufacturer's instructions with hE47^{WT}-IRES-eGFP, hE47^{R558K}-IRES-eGFP or pCAGGs-IRES-eGFP control plasmids (1.5 µg). For p57(KIP2) overexpression experiments, wild-type or E47$^{-/-}$ embryonic NSCs were transfected by electroporation using the Mouse Neural Stem Cell Nucleofector Kit (Lonza) following manufacturer's instructions with mp57(KIP2)-IRES-eGFP or pCAGGs-IRES-eGFP control plasmids (1.5 µg).

Immunocytochemistry

Immunocytochemistry was performed as described previously (Schachtrup et al., 2015) and further details are described in the supplementary Materials and Methods.

Neurite outgrowth assay

Neurite outgrowth assays were performed as previously described using electroporated embryonic NSCs (Schachtrup et al., 2010). Details of the neurite outgrowth assay and analysis are described in the supplementary Materials and Methods.

RNA isolation and quantitative PCR

RNA was isolated from primary embryonic NSCs and quantitative PCR was performed as described previously (Schachtrup et al., 2010). Primer pairs used are described in the supplementary Materials and Methods.

RNA sequencing (RNA-Seq)

RNA isolation from primary embryonic E12$^{-/-}$, and E47$^{-/-}$ NSCs and respective littermate controls at 14.5 was performed as described previously (Schachtrup et al., 2010). The quality of the RNA was verified using an Agilent 2100 Bioanalyzer with RNA 6000Nano Reagents (Agilent Technologies). Library preparation and rRNA depletion was performed using the TruSeq Stranded mRNA Library Prep Kit (Illumina) starting with 500 ng RNA as input for each sample. Libraries were sequenced on the Illumina HiSeq4000. Sequencing quality was assessed with FastQC (http://www.bioinformatics.babraham.ac.uk/projects/fastqc/). The reads were mapped to the mouse genome mm9 (Ensembl build 37.67) and reads per gene counted using STAR (Dobin, 2013) with the following settings: –outFilterType BySJout –outFilterMultimapNmax 20 –alignSJoverhangMin 8 – alignSJDBoverhangMin 1 –outFilterMismatchNmax 999 –outFilter MismatchNoverLmax 0.04 –alignIntronMin 20 –alignIntronMax 1000000 –alignMatesGapMax 100000 –quantMode GeneCounts. The gene annotation information was obtained from Ensembl (build 37.67). Gene count normalization and differential expression analysis was performed using DESeq2 (Love et al., 2014). For gene annotation, biomaRt was used (Durinck et al., 2009). Functional enrichment according to gene ontology was carried out using clusterProfiler (Yu et al., 2012).

Chromatin immunoprecipitation sequencing (ChIP-Seq)

Chromatin immunoprecipitation (ChIP) assays were performed as described (Beck et al., 2009). Details on the ChIP procedure and antibodies used are described in the supplementary Materials and Methods. Purified chromatin was analyzed by high-throughput DNA sequencing on an Illumina HiSeq 3000 as described previously (Uhlenhaut et al., 2013). Reads were aligned to the mouse mm9 reference genome using BWA-MEM version 0.7.13 (Li, 2013 preprint) and PCR duplicates removed using Picard Tools version 1.119 (http://picard.sourceforge.net/). For the visualization of the tracks, mapped reads were converted to bedGraph using the HOMER software suite version 4.8.3 (Heinz et al., 2010) and visualized in the UCSC genome browser (Kent et al., 2002). Peaks were called using MACS2 version 2.1.0 (Zhang et al., 2008) and Gene Ontology analysis performed with GREAT (McLean et al., 2010). Motif discovery and read distribution analysis around E2A peaks was conducted with HOMER. The binding profiles of NeuroD2 (GSE67539) (Bayam et al., 2015) and p300 (GSE42881) (Visel et al., 2013), as well as the H3K4Me1, H3K4Me3, H3K27Ac modification profile (GSE29218) (Shen et al., 2012), were obtained from GEO (Edgar et al., 2002).

Luciferase reporter transactivation assays

The luciferase reporter construct was generated by cloning three putative *Cdkn1c* regulatory elements defined by E2A binding, termed *Cdkn1c* intron (chr7: 150,587,437-150,587,805), *Cdkn1c* downstream (chr7: 150,614,405-150,614,750) and *Cdkn1c* distal intergenic (chr7: 150,623,726-150,624,250), into the pGL3-Admlp2 plasmid (Sayegh et al., 2003). Each fragment was isolated by PCR amplification using C57BL/6J mouse genomic DNA. Details of the luciferase assay procedure and primers used for cloning of reporter constructs are described in the supplementary Materials and Methods.

Co-immunoprecipitation

For endogenous co-immunoprecipitation, cell lysates of primary embryonic NSC cultures were incubated with rabbit anti-mouse E2A antibody (5 µg; sc-349X, Santa Cruz Biotechnology) bound to A-agarose beads for 4 h at 4°C. Details of co-immunoprecipitation are provided in the supplementary Materials and Methods.

Immunoblots

For detection of E47 and E12 expression in wild-type, E47$^{-/-}$ and E12$^{-/-}$ embryonic NSCs, primary cells cultured in proliferation medium were harvested. To detect E12 and E47 expression in wild-type NSCs under proliferating and differentiating conditions, primary cells were cultured in NSC proliferation medium and in NSC differentiation medium for various times. For expression analysis of E47 and E12 in primary NSCs and human E47 and GFP in electroporated embryonic NSCs from wild-type mice, protein extracts were sampled and separated by electrophoresis on 8% and 10% SDS-PAGE gels as described previously (Schachtrup et al., 2010). Antibodies used are described in the supplementary Materials and Methods.

EdU labeling regime

To analyze relative cell cycle length of embryonic NSCs in the cortex, EdU (30 mg/kg body weight, Thermo Fisher) was injected intraperitoneally into

pregnant dams at E12.5 or E14.5. Cumulative EdU labeling of E47$^{-/-}$ and wild-type littermate mouse embryos (C57BL/6 background) at E14.5 was performed by repeated intraperitoneal injections (2 h intervals) into pregnant mice as previously described (Calegari et al., 2005). Relative changes in cell cycle length were assessed by EdU/Ki67 dual immunolabeling of embryonic mouse brain sections collected 2 h and 6 h after EdU injection. The total number of EdU^{+}/Ki67^{+} cells was counted within the VZ and SVZ (Mairet-Coello et al., 2012).

In utero electroporation

Plasmid DNA for electroporation was generated under endotoxin-free conditions using the EndoFree Plasmid Maxi Kit (Qiagen). *In utero* electroporation was performed as previously described (Knuckles et al., 2012). DNA constructs were injected into the lateral ventricles of each embryo at E13.5 of pregnancy in C57BL/6J mice and the embryos were allowed to develop until E15.5 before isolation. Details of the *in utero* electroporation procedure are described in the supplementary Materials and Methods.

Microscopy and imaging analysis

Images were collected using either an Axioplan 2 Imaging epifluorescence microscope, an AxioImager.M2 epifluorescence microscope, a TCS SP8 confocal laser scanning microscope or a Leica DM LED Fluo inverted microscope. Details on microscopy, image processing and quantification are described in the supplementary Materials and Methods.

Statistical analysis

Data are shown as mean±s.e.m. Differences between groups were analyzed by one-way ANOVA followed by Bonferroni's post-test for multiple comparisons. Differences between isolated pairs were examined using Student's *t*-test.

Acknowledgements

We thank Elisabeth Graf for critical help in library generations and sequencing, and Meike Ast-Dumbach for outstanding technical assistance.

Competing interests

The authors declare no competing or financial interests.

Author contributions

Conceptualization: V.T., N.H.U., C.S.; Methodology: S.P., Y.-H.C., C.B., F.G., R.B., K.M., M.H., V.T., K.S., N.H.U., C.S.; Formal analysis: S.P., Y.-H.C., C.B., F.G., R.B., K.M., M.H., V.T., K.S., N.H.U., C.S.; Investigation: S.P., Y.-H.C., C.B., V.T., K.S., C.S.; Resources: S.J.A., C.S.; Writing - original draft: C.S.; Writing - review & editing: C.S.; Supervision: C.S.

Funding

This work was supported by the Fill in the Gap fellowship (Medical Faculty Freiburg) to S.P., by the International Graduate Academy Fellowship (State Baden-Württemberg) to C.B., by a Deutscher Akademischer Austauschdienst fellowship to K.M., by a Deutsche Forschungsgemeinschaft Emmy Noether Programme (AR732/1-1 to S.J.A.), by the Bundesministerium für Bildung und Forschung (BMBF 01EO1303 to K.S.), by the Deutsche Forschungsgemeinschaft Emmy Noether Programme (UH275/1-1 to N.H.U.) and by a Deutsche Forschungsgemeinschaft grant (SCHA 1442/5-1 to C.S.).

Data availability

ChIP-Seq and RNA-Seq data reported in this paper are available at NCBI Gene expression Omnibus with accession numbers GSE88991 (ChIP-Seq) and GSE104065 (RNA-Seq).

Supplementary information

Supplementary information available online at
http://dev.biologists.org/lookup/doi/10.1242/dev.145698.supplemental

References

Arnold, S. J., Sugnaseelan, J., Groszer, M., Srinivas, S. and Robertson, E. J. (2009). Generation and analysis of a mouse line harboring GFP in the Eomes/Tbr2 locus. *Genesis* **47**, 775-781.

Bayam, E., Sahin, G. S., Guzelsoy, G., Guner, G., Kabakcioglu, A. and Ince-Dunn, G. (2015). Genome-wide target analysis of NEUROD2 provides new insights into regulation of cortical projection neuron migration and differentiation. *BMC Genomics* **16**, 681.

Beck, K., Peak, M. M., Ota, T., Nemazee, D. and Murre, C. (2009). Distinct roles for E12 and E47 in B cell specification and the sequential rearrangement of immunoglobulin light chain loci. *J. Exp. Med.* **206**, 2271-2284.

Bedogni, F., Hodge, R. D., Elsen, G. E., Nelson, B. R., Daza, R. A. M., Beyer, R. P., Bammler, T. K., Rubenstein, J. L. R. and Hevner, R. F. (2010). Tbr1 regulates regional and laminar identity of postmitotic neurons in developing neocortex. *Proc. Natl. Acad. Sci. USA* **107**, 13129-13134.

Bohrer, C., Pfurr, S., Mammadzada, K., Schildge, S., Plappert, L., Hils, M., Pous, L., Rauch, K. S., Dumit, V. I., Pfeifer, D. et al. (2015). The balance of Id3 and E47 determines neural stem/precursor cell differentiation into astrocytes. *EMBO J.* **34**, 2804-2819.

Borriello, A., Caldarelli, I., Bencivenga, D., Criscuolo, M., Cucciolla, V., Tramontano, A., Oliva, A., Perrotta, S. and Della Ragione, F. (2011). p57Kip2 and cancer: time for a critical appraisal. *Mol. Cancer Res.* **9**, 1269-1284.

Bronicki, L. M., Belanger, G. and Jasmin, B. J. (2012). Characterization of multiple exon 1 variants in mammalian HuD mRNA and neuron-specific transcriptional control via neurogenin 2. *J. Neurosci.* **32**, 11164-11175.

Calegari, F. and Huttner, W. B. (2003). An inhibition of cyclin-dependent kinases that lengthens, but does not arrest, neuroepithelial cell cycle induces premature neurogenesis. *J. Cell Sci.* **116**, 4947-4955.

Calegari, F., Haubensak, W., Haffner, C. and Huttner, W. B. (2005). Selective lengthening of the cell cycle in the neurogenic subpopulation of neural progenitor cells during mouse brain development. *J. Neurosci.* **25**, 6533-6538.

Casarosa, S., Fode, C. and Guillemot, F. (1999). Mash1 regulates neurogenesis in the ventral telencephalon. *Development* **126**, 525-534.

Castro, D. S., Martynoga, B., Parras, C., Ramesh, V., Pacary, E., Johnston, C., Drechsel, D., Lebel-Potter, M., Garcia, L. G., Hunt, C. et al. (2011). A novel function of the proneural factor Ascl1 in progenitor proliferation identified by genome-wide characterization of its targets. *Genes Dev.* **25**, 930-945.

Deriziotis, P., O'Roak, B. J., Graham, S. A., Estruch, S. B., Dimitropoulou, D., Bernier, R. A., Gerdts, J., Shendure, J., Eichler, E. E. and Fisher, S. E. (2014). De novo TBR1 mutations in sporadic autism disrupt protein functions. *Nat. Commun.* **5**, 4954.

Duquesnes, N., Callot, C., Jeannot, P., Daburon, V., Nakayama, K. I., Manenti, S., Davy, A. and Besson, A. (2016). p57^{Kip2} knock-in mouse reveals CDK-independent contribution in the development of Beckwith-Wiedemann syndrome. *J. Pathol.* **239**, 250-261.

Dobin, A. (2013) STAR: ultrafast universal RNA-seq aligner. *Bioinformatics* **29**, 15-21.

Durinck, S., Spellman, P. T., Birney, E. and Huber, W. (2009). Mapping identifiers for the integration of genomic datasets with the R/Bioconductor package biomaRt. *Nat. Protoc.* **4**, 1184-1191.

Edgar, R., Domrachev, M. and Lash, A. E. (2002). Gene Expression Omnibus: NCBI gene expression and hybridization array data repository. *Nucleic Acids Res.* **30**, 207-210.

Eggermann, T., Binder, G., Brioude, F., Maher, E. R., Lapunzina, P., Cubellis, M. V., Bergadá, I., Prawitt, D. and Begemann, M. (2014). CDKN1C mutations: two sides of the same coin. *Trends Mol. Med.* **20**, 614-622.

Fang, W.-Q., Chen, W.-W., Jiang, L., Liu, K., Yung, W.-H., Fu, A. K. Y. and Ip, N. Y. (2014). Overproduction of upper-layer neurons in the neocortex leads to autism-like features in mice. *Cell Rep.* **9**, 1635-1643.

Fode, C., Ma, Q., Casarosa, S., Ang, S. L., Anderson, D. J. and Guillemot, F. (2000). A role for neural determination genes in specifying the dorsoventral identity of telencephalic neurons. *Genes Dev.* **14**, 67-80.

Furutachi, S., Matsumoto, A., Nakayama, K. I. and Gotoh, Y. (2013). p57 controls adult neural stem cell quiescence and modulates the pace of lifelong neurogenesis. *EMBO J.* **32**, 970-981.

Furutachi, S., Miya, H., Watanabe, T., Kawai, H., Yamasaki, N., Harada, Y., Imayoshi, I., Nelson, M., Nakayama, K. I., Hirabayashi, Y. et al. (2015). Slowly dividing neural progenitors are an embryonic origin of adult neural stem cells. *Nat. Neurosci.* **18**, 657-665.

Gow, C.-H., Guo, C., Wang, D., Hu, Q. and Zhang, J. (2014). Differential involvement of E2A-corepressor interactions in distinct leukemogenic pathways. *Nucleic Acids Res.* **42**, 137-152.

Gradwohl, G., Fode, C. and Guillemot, F. (1996). Restricted expression of a novel murine atonal-related bHLH protein in undifferentiated neural precursors. *Dev. Biol.* **180**, 227-241.

Guo, H., Tian, T., Nan, K. and Wang, W. (2010). p57: a multifunctional protein in cancer (review). *Int. J. Oncol.* **36**, 1321-1329.

Hatanaka, Y., Namikawa, T., Yamauchi, K. and Kawaguchi, Y. (2016). Cortical divergent projections in mice originate from two sequentially generated, distinct populations of excitatory cortical neurons with different initial axonal outgrowth characteristics. *Cereb. Cortex* **26**, 2257-2270.

Heinz, S., Benner, C., Spann, N., Bertolino, E., Lin, Y. C., Laslo, P., Cheng, J. X., Murre, C., Singh, H. and Glass, C. K. (2010). Simple combinations of lineage-determining transcription factors prime cis-regulatory elements required for macrophage and B cell identities. *Mol. Cell* **38**, 576-589.

Development (2017) 144, 3917-3931 doi:10.1242/dev.145698

Hendzel, M. J., Wei, Y., Mancini, M. A., Van Hooser, A., Ranalli, T., Brinkley, B. R., Bazett-Jones, D. P. and Allis, C. D. (1997). Mitosis-specific phosphorylation of histone H3 initiates primarily within pericentromeric heterochromatin during G2 and spreads in an ordered fashion coincident with mitotic chromosome condensation. *Chromosoma* **106**, 348-360.

Heng, J. I.-T., Nguyen, L., Castro, D. S., Zimmer, C., Wildner, H., Armant, O., Skowronska-Krawczyk, D., Bedogni, F., Matter, J.-M., Hevner, R. et al. (2008). Neurogenin 2 controls cortical neuron migration through regulation of Rnd2. *Nature* **455**, 114-118.

Huang, T.-N., Chuang, H.-C., Chou, W.-H., Chen, C.-Y., Wang, H.-F., Chou, S.-J. and Hsueh, Y.-P. (2014). Tbr1 haploinsufficiency impairs amygdalar axonal projections and results in cognitive abnormality. *Nat. Neurosci.* **17**, 240-247.

Imayoshi, I. and Kageyama, R. (2014). bHLH factors in self-renewal, multipotency, and fate choice of neural progenitor cells. *Neuron* **82**, 9-23.

Ince-Dunn, G., Hall, B. J., Hu, S.-C., Ripley, B., Huganir, R. L., Olson, J. M., Tapscott, S. J. and Ghosh, A. (2006). Regulation of thalamocortical patterning and synaptic maturation by NeuroD2. *Neuron* **49**, 683-695.

John, R. M., Ainscough, J. F., Barton, S. C. and Surani, M. A. (2001). Distant *cis*-elements regulate imprinted expression of the mouse *p57^{Kip2}*(*Cdkn1c*)gene: implications for the human disorder, Beckwith–Wiedemann syndrome. *Hum. Mol. Genet.* **10**, 1601-1609.

Joseph, B., Andersson, E. R., Vlachos, P., Södersten, E., Liu, L., Teixeira, A. I. and Hermanson, O. (2009). p57Kip2 is a repressor of Mash1 activity and neuronal differentiation in neural stem cells. *Cell Death Differ.* **16**, 1256-1265.

Kent, W. J., Sugnet, C. W., Furey, T. S., Roskin, K. M., Pringle, T. H., Zahler, A. M. and Haussler, D. (2002). The human genome browser at UCSC. *Genome Res.* **12**, 996-1006.

Knuckles, P., Vogt, M. A., Lugert, S., Milo, M., Chong, M. M. W., Hautbergue, G. M., Wilson, S. A., Littman, D. R. and Taylor, V. (2012). Drosha regulates neurogenesis by controlling neurogenin 2 expression independent of microRNAs. *Nat. Neurosci.* **15**, 962-969.

Kovach, C., Dixit, R., Li, S., Mattar, P., Wilkinson, G., Elsen, G. E., Kurrasch, D. M., Hevner, R. F. and Schuurmans, C. (2013). Neurog2 simultaneously activates and represses alternative gene expression programs in the developing neocortex. *Cereb. Cortex* **23**, 1884-1900.

Kwan, K. Y., Lam, M. M. S., Krsnik, Z., Kawasawa, Y. I., Lefebvre, V. and Sestan, N. (2008). SOX5 postmitotically regulates migration, postmigratory differentiation, and projections of subplate and deep-layer neocortical neurons. *Proc. Natl. Acad. Sci. USA* **105**, 16021-16026.

Kwan, K. Y., Sestan, N. and Anton, E. S. (2012). Transcriptional co-regulation of neuronal migration and laminar identity in the neocortex. *Development* **139**, 1535-1546.

Lange, C., Huttner, W. B. and Calegari, F. (2009). Cdk4/cyclinD1 overexpression in neural stem cells shortens G1, delays neurogenesis, and promotes the generation and expansion of basal progenitors. *Cell Stem Cell* **5**, 320-331.

Lee, J. E. (1997). Basic helix-loop-helix genes in neural development. *Curr. Opin. Neurobiol.* **7**, 13-20.

Li, H. (2013). Aligning sequence reads, clone sequences and assembly contigs with BWA-MEM. *arXiv*:1303.3997.

Li, S., Mattar, P., Zinyk, D., Singh, K., Chaturvedi, C.-P., Kovach, C., Dixit, R., Kurrasch, D. M., Ma, Y.-C., Chan, J. A. et al. (2012). GSK3 temporally regulates neurogenin 2 proneural activity in the neocortex. *J. Neurosci.* **32**, 7791-7805.

Lin, Y. C., Jhunjhunwala, S., Benner, C., Heinz, S., Welinder, E., Mansson, R., Sigvardsson, M., Hagman, J., Espinoza, C. A., Dutkowski, J. et al. (2010). A global network of transcription factors, involving E2A, EBF1 and Foxo1, that orchestrates B cell fate. *Nat. Immunol.* **11**, 635-643.

Love, M. I., Huber, W. and Anders, S. (2014). Moderated estimation of fold change and dispersion for RNA-seq data with DESeq2. *Genome Biol.* **15**, 550.

Mairet-Coello, G., Tury, A., Van Buskirk, E., Robinson, K., Genestine, M. and DiCicco-Bloom, E. (2012). p57^{KIP2} regulates radial glia and intermediate precursor cell cycle dynamics and lower layer neurogenesis in developing cerebral cortex. *Development* **139**, 475-487.

Marthiens, V., Kazanis, I., Moss, L., Long, K. and Ffrench-Constant, C. (2010). Adhesion molecules in the stem cell niche–more than just staying in shape? *J. Cell Sci.* **123**, 1613-1622.

Martynoga, B., Morrison, H., Price, D. J. and Mason, J. O. (2005). Foxg1 is required for specification of ventral telencephalon and region-specific regulation of dorsal telencephalic precursor proliferation and apoptosis. *Dev. Biol.* **283**, 113-127.

McLean, C. Y., Bristor, D., Hiller, M., Clarke, S. L., Schaar, B. T., Lowe, C. B., Wenger, A. M. and Bejerano, G. (2010). GREAT improves functional interpretation of cis-regulatory regions. *Nat. Biotechnol.* **28**, 495-501.

Molyneaux, B. J., Arlotta, P., Menezes, J. R. L. and Macklis, J. D. (2007). Neuronal subtype specification in the cerebral cortex. *Nat. Rev. Neurosci.* **8**, 427-437.

Molyneaux, B. J., Goff, L. A., Brettler, A. C., Chen, H.-H., Brown, J. R., Hrvatin, S., Rinn, J. L. and Arlotta, P. (2015). DeCoN: genome-wide analysis of in vivo transcriptional dynamics during pyramidal neuron fate selection in neocortex. *Neuron* **85**, 275-288.

Murre, C. (2005). Helix-loop-helix proteins and lymphocyte development. *Nat. Immunol.* **6**, 1079-1086.

Murre, C., McCaw, P. S. and Baltimore, D. (1989). A new DNA binding and dimerization motif in immunoglobulin enhancer binding, daughterless, MyoD, and myc proteins. *Cell* **56**, 777-783.

Murre, C., Bain, G., van Dijk, M. A., Engel, I., Furnari, B. A., Massari, M. E., Matthews, J. R., Quong, M. W., Rivera, R. R. and Stuiver, M. H. (1994). Structure and function of helix-loop-helix proteins. *Biochim. Biophys. Acta* **1218**, 129-135.

Nam, H. S. and Benezra, R. (2009). High levels of Id1 expression define B1 type adult neural stem cells. *Cell Stem Cell* **5**, 515-526.

Nieto, M., Schuurmans, C., Britz, O. and Guillemot, F. (2001). Neural bHLH genes control the neuronal versus glial fate decision in cortical progenitors. *Neuron* **29**, 401-413.

Notwell, J. H., Heavner, W. E., Darbandi, S. F., Katzman, S., McKenna, W. L., Ortiz-Londono, C. F., Tastad, D., Eckler, M. J., Rubenstein, J. L. R., McConnell, S. K. et al. (2016). TBR1 regulates autism risk genes in the developing neocortex. *Genome Res.* **26**, 1013-1022.

Pagliuca, A., Gallo, P., De Luca, P. and Lania, L. (2000). Class A helix-loop-helix proteins are positive regulators of several cyclin-dependent kinase inhibitors' promoter activity and negatively affect cell growth. *Cancer Res.* **60**, 1376-1382.

Pérez-Moreno, M. A., Locascio, A., Rodrigo, I., Dhondt, G., Portillo, F., Nieto, M. A. and Cano, A. (2001). A new role for E12/E47 in the repression of E-cadherin expression and epithelial-mesenchymal transitions. *J. Biol. Chem.* **276**, 27424-27431.

Pinto, L. and Gotz, M. (2007). Radial glial cell heterogeneity–the source of diverse progeny in the CNS. *Prog. Neurobiol.* **83**, 2-23.

Prabhu, S., Ignatova, A., Park, S. T. and Sun, X. H. (1997). Regulation of the expression of cyclin-dependent kinase inhibitor p21 by E2A and Id proteins. *Mol. Cell. Biol.* **17**, 5888-5896.

Ravanpay, A. C. and Olson, J. M. (2008). E protein dosage influences brain development more than family member identity. *J. Neurosci. Res.* **86**, 1472-1481.

Reynolds, B. A. and Weiss, S. (1992). Generation of neurons and astrocytes from isolated cells of the adult mammalian central nervous system. *Science* **255**, 1707-1710.

Roberts, V. J., Steenbergen, R. and Murre, C. (1993). Localization of E2A mRNA expression in developing and adult rat tissues. *Proc. Natl. Acad. Sci. USA* **90**, 7583-7587.

Rolando, C., Erni, A., Grison, A., Beattie, R., Engler, A., Gokhale, P. J., Milo, M., Wegleiter, T., Jessberger, S. and Taylor, V. (2016). Multipotency of adult hippocampal NSCs in vivo is restricted by Drosha/NFIB. *Cell Stem Cell* **19**, 653-662.

Ross, S. E., Greenberg, M. E. and Stiles, C. D. (2003). Basic helix-loop-helix factors in cortical development. *Neuron* **39**, 13-25.

Rothschild, G., Zhao, X., Iavarone, A. and Lasorella, A. (2006). E Proteins and Id2 converge on p57Kip2 to regulate cell cycle in neural cells. *Mol. Cell. Biol.* **26**, 4351-4361.

Salomoni, P. and Calegari, F. (2010). Cell cycle control of mammalian neural stem cells: putting a speed limit on G1. *Trends Cell Biol.* **20**, 233-243.

Sanda, T., Lawton, L. N., Barrasa, M. I., Fan, Z. P., Kohlhammer, H., Gutierrez, A., Ma, W., Tatarek, J., Ahn, Y., Kelliher, M. A. et al. (2012). Core transcriptional regulatory circuit controlled by the TAL1 complex in human T cell acute lymphoblastic leukemia. *Cancer Cell* **22**, 209-221.

Sayegh, C. E., Quong, M. W., Agata, Y. and Murre, C. (2003). E-proteins directly regulate expression of activation-induced deaminase in mature B cells. *Nat. Immunol.* **4**, 586-593.

Schachtrup, C., Ryu, J. K., Helmrick, M. J., Vagena, E., Galanakis, D. K., Degen, J. L., Margolis, R. U. and Akassoglou, K. (2010). Fibrinogen triggers astrocyte scar formation by promoting the availability of active TGF-beta after vascular damage. *J. Neurosci.* **30**, 5843-5854.

Schachtrup, C., Ryu, J. K., Mammadzada, K., Khan, A. S., Carlton, P. M., Perez, A., Christian, F., Le Moan, N., Vagena, E., Baeza-Raja, B. et al. (2015). Nuclear pore complex remodeling by p75(NTR) cleavage controls TGF-beta signaling and astrocyte functions. *Nat. Neurosci.* **18**, 1077-1080.

Schuurmans, C., Armant, O., Nieto, M., Stenman, J. M., Britz, O., Klenin, N., Brown, C., Langevin, L.-M., Seibt, J., Tang, H. et al. (2004). Sequential phases of cortical specification involve Neurogenin-dependent and -independent pathways. *EMBO J.* **23**, 2892-2902.

Shen, C. P. and Kadesch, T. (1995). B-cell-specific DNA binding by an E47 homodimer. *Mol. Cell. Biol.* **15**, 4518-4524.

Shen, Y., Yue, F., McCleary, D. F., Ye, Z., Edsall, L., Kuan, S., Wagner, U., Dixon, J., Lee, L., Lobanenkov, V. V. et al. (2012). A map of the cis-regulatory sequences in the mouse genome. *Nature* **488**, 116-120.

Sigvardsson, M., O'Riordan, M. and Grosschedl, R. (1997). EBF and E47 collaborate to induce expression of the endogenous immunoglobulin surrogate light chain genes. *Immunity* **7**, 25-36.

Smart, I. H. and Smart, M. (1982). Growth patterns in the lateral wall of the mouse telencephalon: I. Autoradiographic studies of the histogenesis of the isocortex and adjacent areas. *J. Anat.* **134**, 273-298.

Teachenor, R., Beck, K., Wright, L. Y. T., Shen, Z., Briggs, S. P. and Murre, C. (2012). Biochemical and phosphoproteomic analysis of the helix-loop-helix protein E47. *Mol. Cell. Biol.* **32**, 1671-1682.

Telley, L., Govindan, S., Prados, J., Stevant, I., Nef, S., Dermitzakis, E., Dayer, A. and Jabaudon, D. (2016). Sequential transcriptional waves direct the differentiation of newborn neurons in the mouse neocortex. *Science* **351**, 1443-1446.

Tury, A., Mairet-Coello, G. and DiCicco-Bloom, E. (2011). The cyclin-dependent kinase inhibitor p57Kip2 regulates cell cycle exit, differentiation, and migration of embryonic cerebral cortical precursors. *Cereb. Cortex* **21**, 1840-1856.

Tury, A., Mairet-Coello, G. and DiCicco-Bloom, E. (2012). The multiple roles of the cyclin-dependent kinase inhibitory protein $p57^{KIP2}$ in cerebral cortical neurogenesis. *Dev. Neurobiol.* **72**, 821-842.

Uhlenhaut, N. H., Barish, G. D., Yu, R. T., Downes, M., Karunasiri, M., Liddle, C., Schwalie, P., Hübner, N. and Evans, R. M. (2013). Insights into negative regulation by the glucocorticoid receptor from genome-wide profiling of inflammatory cistromes. *Mol. Cell* **49**, 158-171.

Vetter, M. (2001). A turn of the helix: preventing the glial fate. *Neuron* **29**, 559-562.

Visel, A., Taher, L., Girgis, H., May, D., Golonzhka, O., Hoch, R. V., McKinsey, G. L., Pattabiraman, K., Silberberg, S. N., Blow, M. J. et al. (2013). A high-resolution enhancer atlas of the developing telencephalon. *Cell* **152**, 895-908.

Vlachos, P. and Joseph, B. (2009). The Cdk inhibitor $p57^{Kip2}$ controls LIM-kinase 1 activity and regulates actin cytoskeleton dynamics. *Oncogene* **28**, 4175-4188.

Voronova, A. and Baltimore, D. (1990). Mutations that disrupt DNA binding and dimer formation in the E47 helix-loop-helix protein map to distinct domains. *Proc. Natl. Acad. Sci. USA* **87**, 4722-4726.

Wang, L.-H. and Baker, N. E. (2015). E proteins and ID proteins: helix-loop-helix partners in development and disease. *Dev. Cell* **35**, 269-280.

Warren, N., Caric, D., Pratt, T., Clausen, J. A., Asavaritikrai, P., Mason, J. O., Hill, R. E. and Price, D. J. (1999). The transcription factor, Pax6, is required for cell proliferation and differentiation in the developing cerebral cortex. *Cereb. Cortex* **9**, 627-635.

Yu, G., Wang, L.-G., Han, Y. and He, Q.-Y. (2012). clusterProfiler: an R package for comparing biological themes among gene clusters. *OMICS* **16**, 284-287.

Zalc, A., Hayashi, S., Auradé, F., Bröhl, D., Chang, T., Mademtzoglou, D., Mourikis, P., Yao, Z., Cao, Y., Birchmeier, C. et al. (2014). Antagonistic regulation of $p57^{kip2}$ by Hes/Hey downstream of Notch signaling and muscle regulatory factors regulates skeletal muscle growth arrest. *Development* **141**, 2780-2790.

Zhang, P., Liégeois, N. J., Wong, C., Finegold, M., Hou, H., Thompson, J. C., Silverman, A., Harper, J. W., DePinho, R. A. and Elledge, S. J. (1997). Altered cell differentiation and proliferation in mice lacking p57KIP2 indicates a role in Beckwith-Wiedemann syndrome. *Nature* **387**, 151-158.

Zhang, Y., Liu, T., Meyer, C. A., Eeckhoute, J., Johnson, D. S., Bernstein, B. E., Nusbaum, C., Myers, R. M., Brown, M., Li, W. et al. (2008). Model-based analysis of ChIP-Seq (MACS). *Genome Biol.* **9**, R137.

Supplementary Materials and Methods

In situ hybridization (ISH)

Nonradioactive ISH was performed on cryosections of wild-type (WT) mice as described previously (Ernsberger et al., 1997) using a *Tcf3* specific probe. For ISH, Digoxigenin (DIG) labeled probes were diluted 1:1000 in hybridization buffer. Hybridization and subsequent washing was performed at 68°C, washing with maleic acid buffer and 0.1% Tween (MABT) was carried out 2 × 30 min before sections were blocked with lamb serum at RT for 1 h. Anti-DIG alkaline phosphatase conjugate was diluted 1:5000. The color reaction was performed overnight at RT using NBT/BCIP Stock Solution (Roche) diluted 1:100. *In situ* probes were *in vitro* transcribed from linearized plasmids at 37°C for 2 h. The following primers were used:

Tcf3 Fwd: 5`-GTCCTGGGTGGATGATGAACC-3`

Tcf3 Rev: 5´-CAACGAAGAAGCTGTGACG-3´

Immunohistochemistry (IHC)

Primary antibodies used for IHC: rabbit anti-E2A (1:1000, sc-349X, Santa Cruz Biotechnology), goat anti-GFP (1:1000, Abcam), rabbit anti-Ki67 (1:500, Abcam), goat anti-Nestin (1:200, Santa Cruz Biotechnology), rabbit anti-NeuN (1:2000, Abcam), rabbit anti-p57(KIP2) (1:500, Sigma P0357), mouse anti-Pax6 (1:50, Developmental Studies Hybridoma Bank), mouse anti-Satb2 (1:500, Abcam), rabbit anti-Tbr1 (1:500, Abcam), rabbit anti-Tbr2 (1:2000, Millipore), rat anti-Tbr2 (1:500, Invitrogen), guinea pig anti-Vglut1 (1:500, Millipore), mouse anti-Mash1 (1:500, BD Bioscience), rat anti-Ctip2 (1:500, Abcam), mouse anti-Sox2 (1:1000, Abcam), rabbit anti-Ngn2 (1:200, Cell

Signaling), mouse anti-neurofilament (1:100, Developmental Study Hybridoma Bank), mouse anti-Tuj-1 (1:200, Millipore), rabbit anti-cleaved caspase-3 (1:100, Cell Signaling), mouse anti-Gad67 (1:1000, Millipore), rabbit anti-Math2 (1:1000, Abcam), mouse anti-NeuroD1 (1:1000, Abcam). Secondary antibodies used were conjugated with fluorescein isothiocyanate (FITC), Alexa Fluor 488 or 594 (1:200, Jackson ImmunoResearch Laboratories). Sections were coverslipped with 4′,6-diamidino-2-phenylindole (DAPI) Fluoromount-G® solution (Southern Biotech).

Immunocytochemistry (ICC)

Primary antibodies used for ICC: rat anti-BrdU (1:300, Abcam), rabbit anti-cleaved caspase-3 (1:100, Cell Signaling), goat anti-GFP (1:1000, Abcam) or mouse anti-Tuj-1 (1:100, Millipore) in 1% BSA/PBS overnight. After three washes in PBS, cells were incubated with an appropriate secondary antibody conjugated with either FITC, Alexa Fluor 488 or 594 (1:200, Jackson ImmunoResearch Laboratories) for 1 h in 1% BSA/PBS at RT, washed in PBS, and mounted with DAPI Fluoromount-G® solution (Southern Biotechnology).

Neurite outgrowth assay

For the neurite outgrowth assays, 125.000 electroporated WT and *E47-/-* cells were cultured in differentiation medium, allowed to extend processes for 48 h (Fig. 7A,B) or for 24 h (Fig 7H,I) and stained for Tuj-1. Neurite outgrowth was determined as the proportion of cells bearing neurites two times longer than the diameter of the cell body, an indication of successful initiation of neurite outgrowth (Schachtrup et al., 2007). The number of neurite-bearing cells was measured from at least 200 GFP+ neurons per

condition. Quantification of cell numbers was performed using ImageJ software (National Institutes of Health).

RNA isolation and quantitative PCR

The following primers were used for quantitative PCR:

E12 Fwd: *5′-GGGAGGAGAAAGAGGATGA-3′*

E12 Rev: *5′-GCTCCGCCTTCTGCTCTG-3′*

E47 Fwd: *5′-GGGAGGAGAAAGAGGATGA-3′*

E47 Rev: *5′-CCGGTCCCTCAGGTCCTTC-3′*

E-cadherin Fwd: *5´-AATGGCGGCAATGCAATCCCAAGA-3´*

E-cadherin Rev: 5´-TGCCACAGACCGATTGTGGAGATA-3´

Gapdh Fwd: 5´-CAAGGCCGAGAATGGGAAG-3′

Gapdh Rev: 5´-GGCCTCACCCCATTTGATGT-3′

Cdkn1a Fwd: 5´- CCT GGTGATGTCCGACCTG-3´

Cdkn1a Rev: 5´- CCATGAGCGCATCGCAATC-3´

Cdkn1b Fwd: 5´- TCAAACGTGAGAGTGTCTAACG-3´

Cdkn1b Rev: 5´- CCGGGCCGAAGAGATTTCTG-3´

Cdkn1c Fwd: 5´-CGAGGAGCAGGACGAGAATC-3´

Cdkn1c Rev: 5´-GAAGAAGTCGTTCGCATTGGC-3′

Chromatin Immunoprecipitation Sequencing (ChIP-Seq)

Embryonic NSCs (approx. 10 x 10^6 cells) were fixed with 1.5 mM ethylene glycol bis[succinimidyl succinate] in DMSO for 20 min at RT, followed by adding

formaldehyde to a final concentration of 1%, incubated for 10 min at RT and finally quenched by 0.2 M glycine. Cells were then lysed and sonicated with a microtip for 10 seconds followed by a 1 min break for 10 cycles. After adding 1% Triton-X to the sonicated lysates, ChIP was performed overnight at 4°C with Dynabeads M-280 Sheep anti-Rabbit IgG (Thermo Fisher, 11203D) linked to either rabbit anti-E2A (1.5 µg, sc-349X, Santa Cruz Biotechnology) or control rabbit anti-IgG (1.5 µg, sc-2027, Santa Cruz Biotechnology). 10% of sonicated suspension was kept as input control. After washing and elution of chromatin-antibody complexes from the beads at 65°C overnight, crosslinking was reversed by proteinase K and RNase digestion. Genomic DNA and DNA from the sonicated input were purified using a PCR Purification Kit (Qiagen).

Luciferase reporter transactivation assays

The reporter constructs were co-transfected with the constitutively active *Renilla reniformis* luciferase producing vector pRL-CMV (Promega) into HEK293T cells by calcium phosphate co-precipitation. Cells were lysed 24 h after transfection using passive lysis buffer (Promega). Luciferase activity was determined in duplicates using a 96-well plate reader (PerkinElmer) with automatic injection of 100 µl substrate and measurement for 10 seconds after a 2 second delay. For measuring *Renilla* luciferase activity, the *Renilla Juice Kit* (PJK) was used as a substrate according to the manufacturer's instructions. Firefly luciferase activity was quantified by using firefly substrate solution containing luciferin. For cloning of the reporter construct the following primers were used:

p57-Intron (p57-I) Fwd: 5′-AGATCTCAAGGGCCCAAGAGAGTGC-3′

p57-Intron (p57-I) Rev: 5′- AGATCTGCCAAACTTCTCTGGCCAAT-3′

p57-Downstream (p57-II) Fwd: 5′- AGATCTGTTCT-CCCGCAAGGACCATT-3′

p57-Downstream (p57-II) Rev: 5′- AGATCTGCAGAGGCAGTCCCATGAAA-3′

p57-Distal Intergenic (p57-III) Fwd: 5′-AGATCTAGGTAGGGATGGTCCCAGAC-3′

p57-Distal Intergenic (p57-III) Rev: 5′-AGATCTGGTCATACACCACAAGGGCA-3′

Immunoblots

The following antibodies were used for Western blotting: mouse anti-E12 (1:5000, BD Pharmingen, Cat.no. 6656/A), mouse anti-E47 (1:6000, BD Pharmingen, Cat.no. 554077), mouse anti-E47 (1:6666, BD Pharmingen, Cat.no. 554199), rabbit anti-GAPDH (1:1000, Cell Signaling), rabbit anti-GFP (1:1000, Cell Signaling).

Co-immunoprecipitation

Co-immunoprecipitation was performed as described (Schachtrup et al., 2015). For endogenous co-immunoprecipitation, cell lysates of primary embryonic NSC cultures were incubated with rabbit anti-mouse E2A antibody (5 µg, sc-349X, Santa Cruz Biotechnology) bound to A-agarose beads for 4 h at 4°C. Cell lysates were probed with the following antibodies: rabbit anti-Limk (1:1000, Cell Signaling), mouse anti-NeuroD1 (1:1000, Abcam), rabbit anti-NeuroD2 (1:1000, Abcam), rabbit anti-Math2 (1:500, Abcam), rabbit anti-Ngn2 (1:500, Santa Cruz), and rabbit anti-Mash1(1:500, Abcam).

***In utero* electroporation**

For *in utero* electroporation, DNA constructs were dissolved in sterile PBS (3-4 µg/µl), mixed with a fast green contrast dye and injected into the lateral ventricles of each

embryo at E13.5 of pregnant C57BL/6J mice using a microinjector and pulled Borosilicate glass capillaries. Electroporation was performed by applying ten pulses of 40 V and a pulse length of 50 ms within a 950 ms interval to the head of each embryo with the anode of the electrode oriented toward the injected side. After injection and electroporation, the uterus was replaced in the body cavity, the muscle and the skin sutured and the embryos were allowed to develop until E15.5 before isolation. The following plasmids were used: pCAGGs-IRES-eGFP and hE47^{WT}-IRES-eGFP.

Microscopy and imaging analysis

Representative images of *E2A* mRNA expression on sagittal brain sections were acquired with an Axioplan 2 Imaging epifluorescence microscope and dry Plan-NEOFLUAR objectives (10x/0,30 NA; 20x/0,50 NA), an Axiocam HRc CCD camera and the AxioVision image analysis software (Carl Zeiss). For quantification analyses of cell populations or immunoreactivity on sagittal brain sections as well as for *in vitro* overexpression assays, BrdU labeling studies, and apoptosis assays, microscopic images were acquired with an AxioImager.M2 epifluorescence microscope and dry Plan-NEOFLUAR objectives (10x/0,30 NA; 20x/0,50 NA; 40x/0,75 NA), an Axiocam HRc CCD camera and the image analysis software ZEN 2012 blue edition (Carl Zeiss). Representative images and images for quantification analyses were acquired with a TCS SP8 confocal laser scanning microscope using the 40x oil immersion objective and the LAS AF image analysis software (Leica). For quantification analyses of neurosphere diameter, microscopic images were acquired with a Leica DM LED Fluo inverted microscope and dry N PLAN objective (5x/0,12 NA) and HI PLAN objective (10x/0,25), a Leica DFC3000 G camera and the image analysis software LAS AF. For quantification

of the number of Tbr1, Satb2, Ctip2, Pax6, Sox2, NeuN, Ngn2, and cleaved caspase-3 cells, we analyzed an area in the caudal neocortex spanning the cortical wall from the ventricular surface to the pia with a width of 40 µm (Satb2, E14.5), 80µm (Sox2, E14.5), 100 µm (NeuN, Ngn2, and Tbr2 at E14.5), 120 µm (Satb2 at E18.5), 150 µm (Satb2 at P3), 200 µm (Tbr1, Pax6, and Ctip2 at E14.5), 374µm (Tbr1 at E18.5), 400 µm (Tbr1 at P3), and 700 µm (cleaved caspase-3). For Tbr1 bin quantification, defined areas as indicated above were subdivided into 10 equal bins along the dorsoventral axis and the number of cells in each bin was determined (Magno et al., 2012). For quantification analysis of p57(KIP2), and neurofilament, we analyzed an area in the caudal neocortex spanning the cortical wall from the ventricular surface to the pia with a width of 145µm (neurofilament at E14.5), 200µm (p57(KIP2) at E12.5), and 500 µm (p57(KIP2) at E14.5). For immunoreactivity analysis of E2A in Pax6+ cells (Fig. 1D), we divided Pax6 labeled VZ into apical region (40µm from the ventricular surface) and basal region (100µm from the apical region) (Kowalczyk et al., 2009). E2A+ cells colocalizing with Pax6 were analyzed in the apical and basal VZ with a width of 250µm. For immunoreactivity analysis of E2A in Ki67+ cells (Fig. 1E), E2A+/Ki67+ cells (10 cells per animal) were randomly selected in the total VZ and the number of pixels with an intensity above a predetermined threshold level was determined as E2Ahigh and E2Alow (Fig. 1D and Fig. 1E). For quantification of the number of GFP+/p57(KIP2)+ cells after *in utero* electroporation, we analyzed an area in the middle neocortex spanning the cortical wall from the ventricular surface to the pia with a width of 80 µm. For quantification of neurite outgrowth after *in utero* electroporation and after electroporation *in vitro*, GFP+ cells with a neurite length twice that long than the diameter of the cell body of the neuron were counted as neurite bearing cells as previously described

(Schachtrup et al., 2007). For *in vivo* and *in vitro* neurite outgrowth analyses after *in utero electroporation* at least 100 GFP+ neurons per condition were measured. For quantification of the number of GFP+ cells after *in utero electroporation*, GFP+ cells were counted in the cortical plate spanning an area with a width of 80 µm (Fig. 6E, cortical plate. For quantification of the number of Ki67+ cells, EdU+/Ki67+, and PH3+ embryonic NSCs for cell proliferation and cell cycle length analyses, we analyzed an area in the caudal neocortex spanning the cortical wall from the ventricular surface to the pia with a width of 100 µm (Ki67+ and EdU+/Ki67+ cells) and 400 µm (pH3+ cells). At least three brain sections per animal were analyzed for cortical quantifications. For proliferation analyses *in vitro*, the diameter of at least 200 neurospheres and 200 BrdU-labeled embryonic NSCs were assessed. For apoptosis assays *in vitro* at least 200 embryonic NSCs per condition were analyzed.

Supplementary References

Ernsberger, U., Patzke, H. and Rohrer, H. (1997). The developmental expression of choline acetyltransferase (ChAT) and the neuropeptide VIP in chick sympathetic neurons: evidence for different regulatory events in cholinergic differentiation. *Mech Dev* **68**, 115-126.

Kowalczyk, T., Pontious, A., Englund, C., Daza, R. A., Bedogni, F., Hodge, R., Attardo, A., Bell, C., Huttner, W. B. and Hevner, R. F. (2009). Intermediate neuronal progenitors (basal progenitors) produce pyramidal-projection neurons for all layers of cerebral cortex. *Cereb Cortex* **19**, 2439-2450.

Magno, L., Oliveira, M. G., Mucha, M., Rubin, A. N. and Kessaris, N. (2012). Multiple embryonic origins of nitric oxide synthase-expressing GABAergic neurons of the neocortex. *Front Neural Circuits* **6**, 65.

Schachtrup, C., Lu, P., Jones, L. L., Lee, J. K., Lu, J., Sachs, B. D., Zheng, B. and Akassoglou, K. (2007). Fibrinogen inhibits neurite outgrowth via beta 3 integrin-mediated phosphorylation of the EGF receptor. *Proc Natl Acad Sci U S A* **104**, 11814-11819.

Schachtrup, C., Ryu, J. K., Mammadzada, K., Khan, A. S., Carlton, P. M., Perez, A., Christian, F., Le Moan, N., Vagena, E., Baeza-Raja, B., et al. (2015). Nuclear pore complex remodeling by p75(NTR) cleavage controls TGF-beta signaling and astrocyte functions. *Nat Neurosci* **18**, 1077-1080.

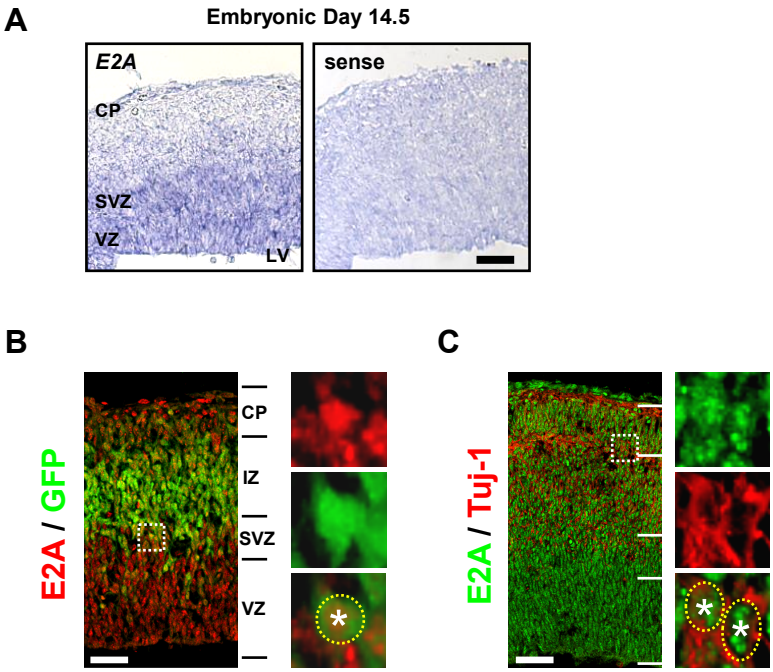

Figure S1. Expression of E2A in intermediate precursor cells and postmitotic neurons during cortical development. (A) *In situ* hybridization of E2A mRNA (blue) using antisense probe (A, left) and a sense control (A, right) of representative sagittal brain sections of C57BL/6 mice at E14.5. Scale bar: 200 µm. (*n* = 3). (B) Immunolabeling for E2A (red) in the cortex in representative sagittal brain sections of Eomes^{GFP} mice at E14.5. Eomes^{GFP} expressing cells can be identified by green fluorescence. Scale bar: 50 µm. (*n* = 3 mice). (C) Immunolabeling for E2A (green) in combination with Tuj-1 (red) in the cortex in representative sagittal brain sections of C57BL/6 mice at E14.5. White boxes indicate representative E2A colocalization with GFP+ (A) and Tuj-1+ (B) cells (high magnification images at the right, respectively). Scale bar: 50 µm. (*n* = 3 mice). Abbreviations: CP, cortical plate; IZ, intermediate zone; SVZ, subventricular zone; VZ, ventricular zone.

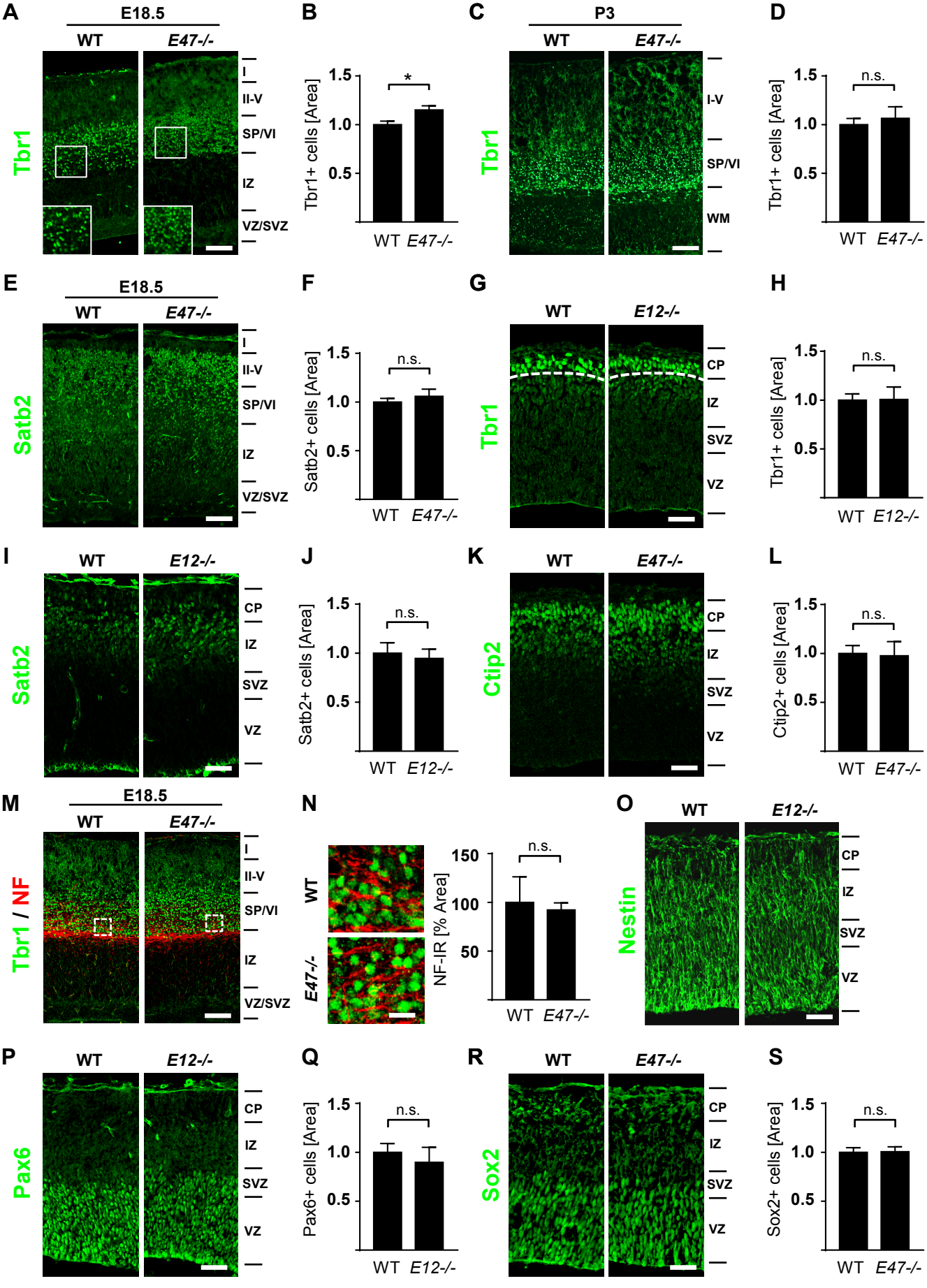

Figure S2. E12 does not regulate deep-layer or upper-layer neurogenesis at E14.5. (A,C) Immunolableing for Tbr1 (green) in sagittal brain sections of *E47-/-* mice compared to WT littermates at E18.5 (A) and P3 (C). Scale bar: 110 µm. (B,D) Quantification of the number of Tbr1+ neurons (n = 4 mice, B; n = 4 WT mice, n = 3 *E47-/-* mice, D). (E) Immunolabeling for Satb2 (green) in sagittal brain sections of *E47-/-* mice compare to WT littermates at E18.5. Scale bar: 110 µm. (F) Quantification of the number of Satb2+ cells (n = 4 mice). (G,I) Immunolabeling for Tbr1 (G, green) and Satb2 (I, green) in sagittal brain sections of *E12-/-* mice compared to WT littermates at E14.5. Scale bar: 40 µm. (H,J) Quantification of the number of Tbr1+ (H) and Satb2+ (J) neurons (n = 5 WT mice, n = 3 *E12-/-* mice, H; n = 4 WT mice, n = 3 *E12-/-* mice, J). (K) Immunolabeling for Ctip2 (green) in the cortex in sagittal sections of *E47-/-* mice at E14.5. Scale bar: 40 µm. (L) Quantification of the number of Ctip2+ subcortical projection neurons in cortical brain sections of *E47-/-* mice and WT littermates at E14.5 (n = 4 WT mice, n = 5 *E47-/-* mice). (M) Immunolabeling for Tbr1 (green) and neurofilament (red) in sagittal brain sections of *E47-/-* mice compared to WT littermates at E18.5. Enlargements of regions indicated by rectangles represent area of quantification. Scale bars: 110 µm (M), 17 µm (N). (N) Quantification of the immunoreactivity of neurofilament (n = 3 mice). (O) Immunolabeling for Nestin (green) in the cortex in representative sagittal sections of *E12-/-* mice at E14.5 (n = 3 mice). Scale bar: 40 µm. (P) Immunolabeling for Pax6 (green) in the cortex in sagittal sections of *E12-/-* mice at E14.5. Scale bar: 40 µm. (Q) Quantification of the number of Pax6+ radial glial cells in cortical brain sections of *E12-/-* mice and WT littermates at E14.5 (n = 5 WT mice, n = 3 *E12-/-* mice). (R) Immunolabeling for Sox2 (green) in the cortex in sagittal sections of *E47-/-* mice at E14.5. Scale bar: 40 µm. (S) Quantification of the number of Sox2+ radial glial and intermediate progenitor cells in cortical brain sections of *E47-/-*

mice and WT littermates at E14.5 (n = 7 WT mice, n = 6 *E47-/-* mice). Bar graphs are mean ± s.e.m. *$P < 0.05$ calculated by Student´s t test. Abbreviations: CP, cortical plate; SP, subplate; IZ, intermediate zone; NF, neurofilament; SVZ, subventricular zone; VZ, ventricular zone, WM, white matter.

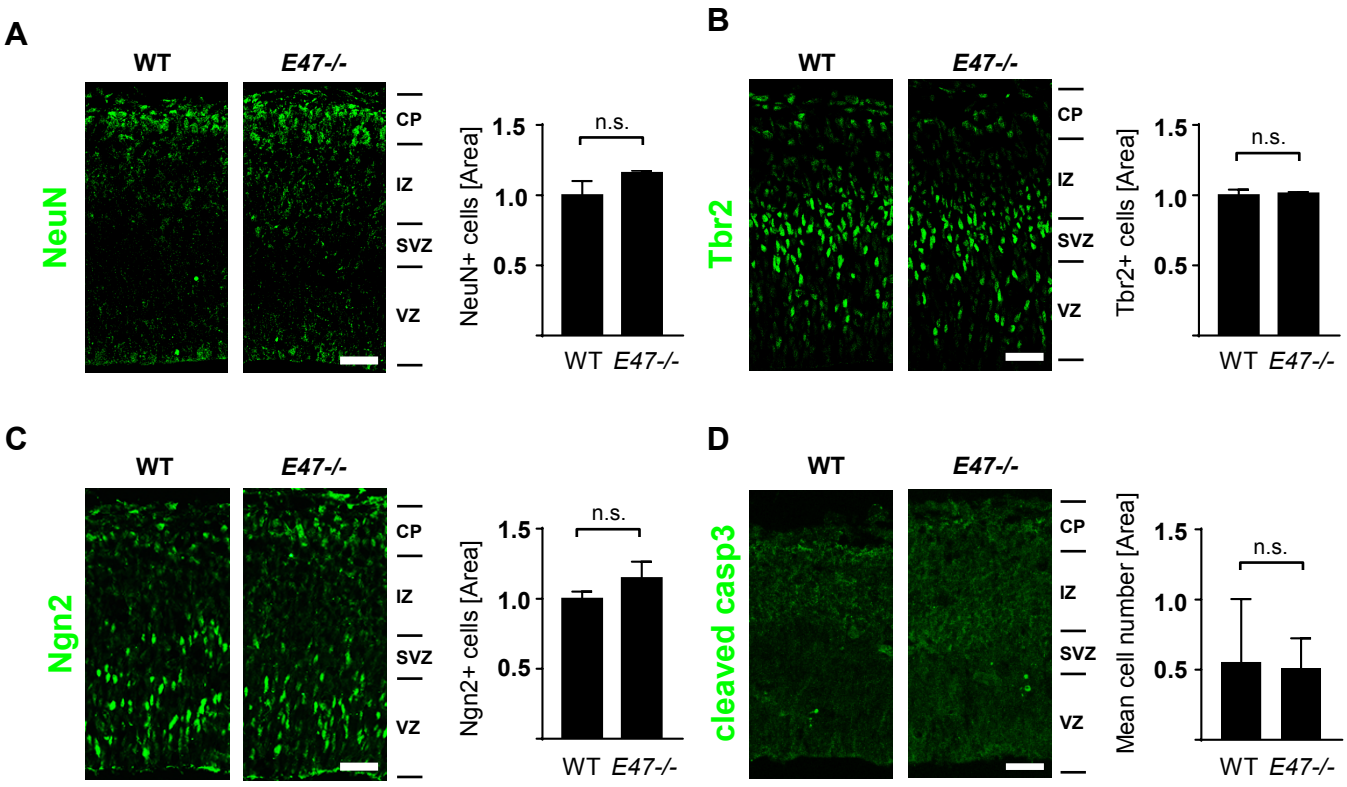

Figure S3. Distribution of intermediate precursor cells and postmitotic neurons in *E47-/-* cortices at E14.5. (A) Immunolabeling for NeuN (green) in the cortex in sagittal brain sections of *E47-/-* mice at E14.5 (left, A) and quantification of NeuN+ cells in the cortical area (right, A). Scale bar: 40 µm. (*n* = 3 mice). (B) Immunolabeling for Tbr2 (green) in the cortex in sagittal brain sections of *E47-/-* mice and WT littermates at E14.5 (left, B) and quantification of Tbr2+ cells in the cortical area (right, B). Scale bar: 40 µm. (*n* = 4 WT mice, *n* = 3 *E47-/-* mice). (C) Immunolabeling for Ngn2 (green) in the cortex in sagittal brain sections of *E47-/-* mice and WT littermates at E14.5 (left, C) and quantification of Ngn2+ cells in the cortical area (right, C). Scale bar: 40 µm. (*n* = 6 WT mice, *n* = 6 *E47-/-* mice). (D) Immunolabeling for cleaved caspase-3 (green) in the cortex in sagittal brain sections of *E47-/-* mice and WT littermates at E14.5 (left, D) and quantification of cleaved caspase-3+ cells in the cortical area (right, D). Scale bar: 40 µm. (*n* = 2 WT mice, *n* = 2 *E47-/-* mice). Bar graphs are mean ± s.e.m. *p*-values were calculated by Student´s *t* test. Abbreviations: CP, cortical plate; IZ, intermediate zone; SVZ, subventricular zone; VZ, ventricular zone.

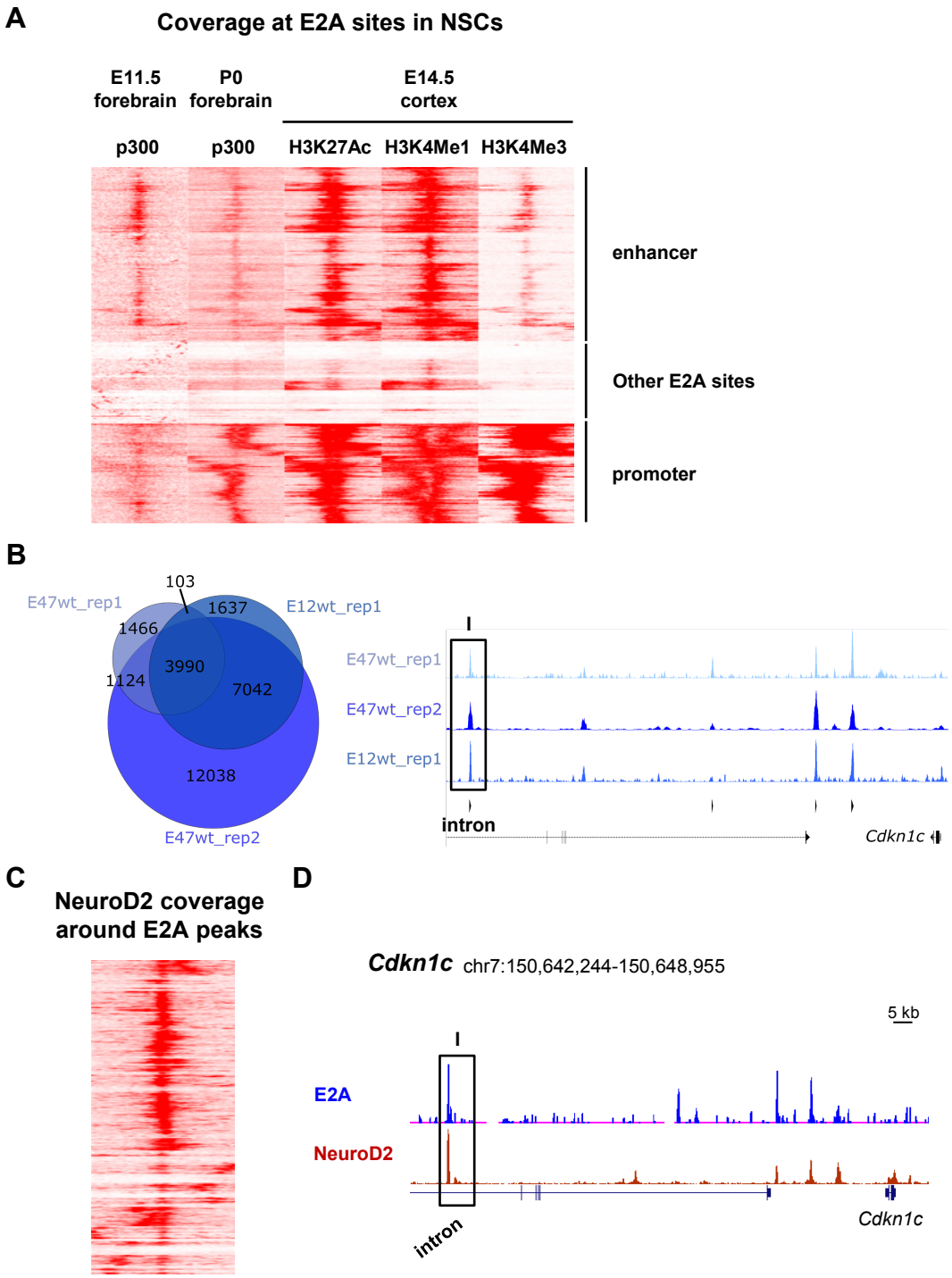

Figure S4. E2A binds predominantly to active enhancer and promoter in neuronal tissue, partially sharing binding sites with NeuroD2. (A) Comparative analysis of genome-wide enrichment of p300 (Visel et al., 2013) and H3K4Me1, H3K4Me3 and H3K27Ac histone marks (Shen et al., 2012) around E2A binding sites in embryonic NSCs (our study). Epigenetic signatures distinguish active enhancers (H3K27Ac/H3K4Me1^{high}/H3K4Me3^{low}) from promoter regions (H3K27Ac/H3K4Me1^{low}/H3K4Me3^{high}). Note that, at promoter regions H3K4Me1 was low and H3K4Me3 was high around the peak center of E2A binding, while H3K4Me1 was preferentially increased in the surrounding regions. (B) E2A ChIP-Seq reproducibility in WT embryonic NSCs. The Venn diagram depicts the E2A binding sites identified in 3 independent ChIP-Seq experiments. Binding sites are called "reproducible" when they were identified in 2 out of 3 experiments (FDR<0.01). The ChIP-Seq tracks for the *Cdkn1c* locus show 4 reproducibly identified E2A binding sites (black arrow heads). One of those being the functional E47 enhancer in the intron of *Kcnq1* (black box I). (C,D) Genome-wide coverage of NeuroD2 binding events (Bayam et al., 2015) around E2A binding sites in embryonic NSCs (C) including the identified poised enhancer p-57 I located in the *Cdkn1c* locus (D).

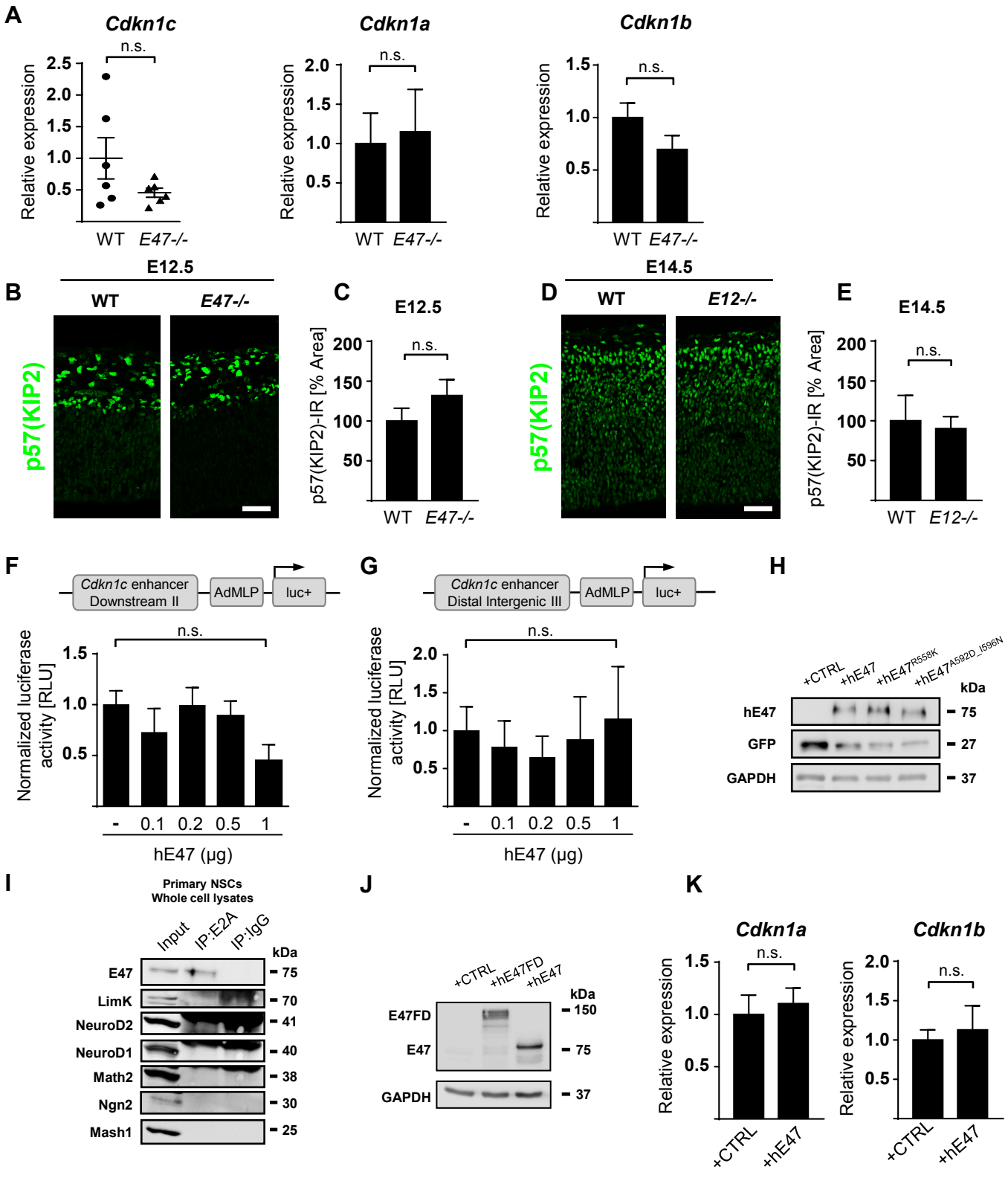

Figure S5. E47 does not regulate mRNA expression of *Cdkn1a* and *Cdkn1b* in embryonic NSCs. (A) Expression of *Cdkn1c*, *Cdkn1a*, and *Cdkn1b* mRNA in embryonic WT and *E47-/-* NSCs under proliferation conditions. Quantitative PCR results are of four independent experiments performed in duplicate. (B) Immunolabeling for p57(KIP2) (green) in sagittal brain sections of *E47-/-* mice compared to WT littermates at E12.5. Scale bar: 40 µm. (C) Quantification of the p57(KIP2) immunoreactivity (*n* = 3 WT mice, *n* = 4 *E47-/-* mice). (D) Immunolabeling for p57(KIP2) (green) in sagittal brain sections of *E12-/-* mice compared to WT littermates at E14.5. Scale bar: 40 µm. (E) Quantification of the p57(KIP2) immunoreactivity (*n* = 3 WT mice, *n* = 3 *E12-/-* mice). (F,G) Luciferase reporter assay in HEK293T cells using the indicated p57(KIP2) luciferase reporter construct (F, *Cdkn1c* enhancer II termed as downstream) and (G, *Cdkn1c* enhancer III termed as distal intergenic). Luciferase reporter assay results are of three independent experiments performed in duplicate. (H) Immunoblot protein expression analysis for E47 in FACS sorted mouse embryonic NSCs 24 h after electroporation with WT hE47^{WT}-IRES-eGFP, mutant hE47^{R558K}-IRES-eGFP and mutant hE47^{A592D_I596N}-IRES-eGFP plasmid. Representative Western blots are shown from two independent experiments. (I) Endogenous coimmunoprecipitation of E47 with potential interaction partners in whole embryonic NSC lysates. Representative immunoblots are shown from two independent experiments. (J) Immunoblot protein expression analysis for hE47 forced homodimer (hE47FD) in HEK293T cells 24 h after transfection with hE47^{FD}-pMIG plasmid. Representative Western blots are shown from two independent experiments. (K) Expression of *Cdkn1a* mRNA (left) and *Cdkn1b* mRNA (right) in embryonic NSCs 24 h after electroporation with hE47^{WT}-IRES-eGFP plasmid in comparison to cells electroporated with pCAGGs-IRES-eGFP control plasmid determined by quantitative PCR and normalized to *GAPDH*. Quantitative PCR results are of six independent experiments performed in duplicate. Bar graphs are mean ± s.e.m. *p*-values were calculated by Student´s *t* test (A,C,E,K) or by one-way ANOVA (F,G)]. Abbreviations: CDKI, cyclin-dependent kinase inhibitor protein; RLU, relative light unit.

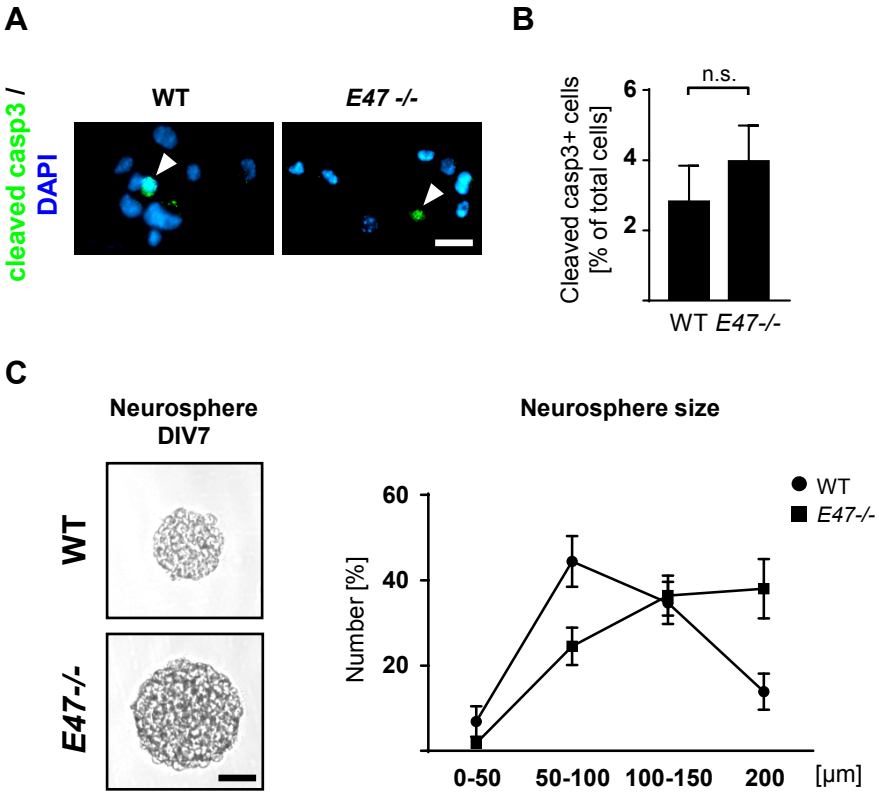

Figure S6. E47-deficiency does not affect apoptotic cell death but neurosphere size of embryonic NSCs *in vitro*. (A,B) Immunolabeling for cleaved caspase-3 (green) of *E47-/-* and WT embryonic NSCs (A) and quantification of cleaved caspase-3+ cells (B). Scale bar: 20 µm. Apoptotic cell death results are of three independent experiments. (C) Distribution of the diameter of individual formed neurospheres from *E47-/-* and WT dissociated primary NSCs after 7 DIV in proliferation medium. *E47-/-* embryonic NSCs formed increased numbers of bigger size neurospheres (200 µm), but less medium size neurospheres (50-100 µm) compared to WT NSCs. Scale bar: 40 µm. Neurosphere size results are of three independent experiments. Values are mean ± s.e.m. *p*-values were calculated by Student´s *t* test (B).

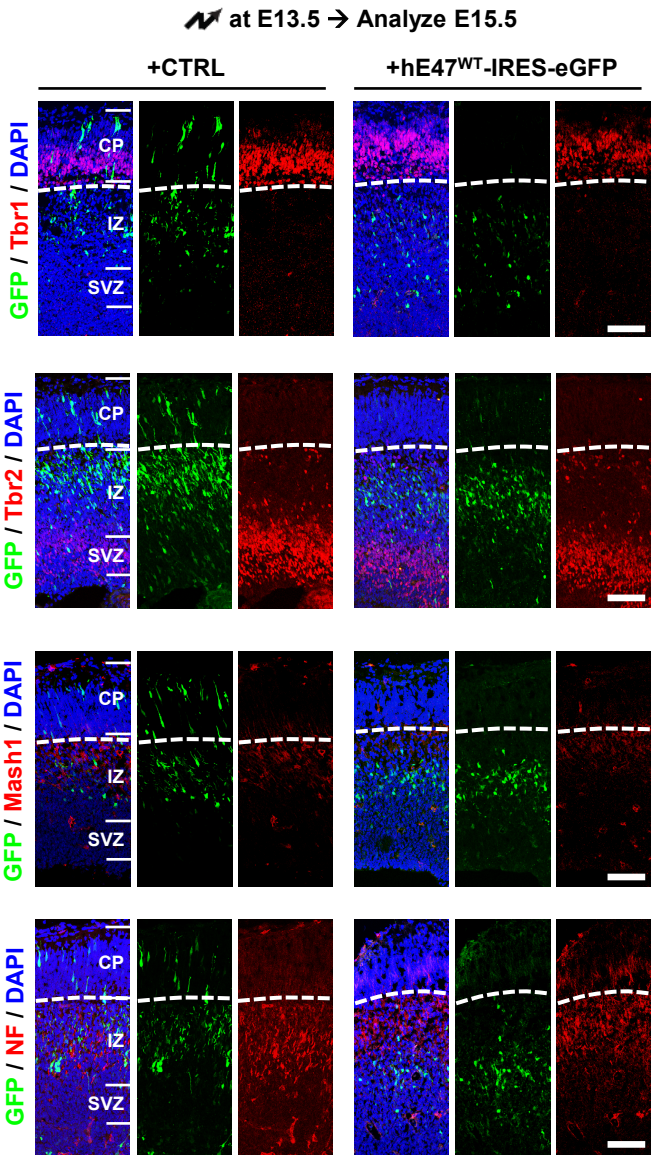

Figure S7. E47 overexpressing cells show a failure in lower layer neuron differentiation. *In utero* electroporation of WT mice at E13.5 with either pCAGGs-IRES-eGFP or hE47^{WT}-IRES-eGFP. Immunolabeling was performed for Tbr1 (red, deep-layer neuron marker, top row), Tbr2 (red, intermediate progenitor cells, second top row), Mash1 (red, ventral telencephalon neuron, second bottom row), neurofilament (red, projecting axons, bottom) in combination with GFP (green, electroporated cells) in sagittal brain sections at E15.5. Scale bars: 80 µm (left), Nuclei are stained with DAPI (blue). Abbreviations: CP, cortical plate; IZ, intermediate zone; NF, neurofilament; SVZ, subventricular zone.

Table S1: Overlapping differentially expressed genes in *E12-/-* and *E47-/-* primary embryonic NSCs having an E2A binding site in WT cells. Depicted are the results from RNA-Seq indicating the fold-change in gene expression as log2 (log2FC) in *E47-/-* or *E12-/-* NSCs, variance between triplicates as P.

Symbol	**log2FC E47-/-**	**P E47-/-**	**log2FC E12-/-**	**P E12-/-**
Tdg	-1.75	5.15E-45	-1.64	1.39E-120
Csmd3	-1.23	7.20E-03	-0.60	2.03E-01
Ckmt1	-1.14	5.40E-03	-0.72	6.99E-02
1190007I07Rik	-1.07	3.65E-05	-1.00	3.40E-04
Adamts3	-1.06	4.05E-04	-0.84	9.06E-12
Col1a1	-1.05	1.87E-01	-1.85	6.19E-13
Plppr5	-0.97	3.13E-03	-0.86	4.49E-04
Pcdh15	-0.96	3.15E-03	-1.32	7.25E-03
Cntn1	-0.90	2.87E-05	-0.96	1.98E-02
Plppr1	-0.90	3.37E-04	-0.97	1.57E-04
Moxd1	-0.86	9.05E-02	-1.45	5.06E-03
Brinp1	-0.86	3.70E-02	-1.18	1.10E-02
Unc5c	-0.84	1.87E-02	-0.80	1.48E-02
Dpp10	-0.83	2.82E-03	-1.20	1.43E-01
Clic5	-0.81	2.06E-02	0.84	2.29E-03
Ptpn5	-0.80	3.94E-03	-0.97	2.86E-03
Grik3	-0.78	2.06E-05	-0.95	1.39E-02
Shisa7	-0.73	8.15E-03	-0.99	1.27E-01

Hmcn1	-0.72	5.81E-02	0.69	2.92E-04
Nkd2	-0.72	7.53E-02	-0.63	6.61E-03
Kcnq2	-0.71	9.02E-02	-1.13	2.10E-02
Gabrb2	-0.70	2.23E-02	-0.85	4.36E-03
Cobl	-0.70	1.82E-01	-0.67	3.18E-02
Spo11	-0.69	1.60E-01	-1.43	6.96E-06
Vat1l	-0.67	9.92E-02	-1.12	9.67E-02
Cntnap5b	-0.66	2.16E-02	-0.74	9.49E-03
B3gat2	-0.66	2.07E-03	-0.74	6.41E-03
Atp10b	-0.66	1.24E-01	-0.88	2.40E-02
Ppfia2	-0.65	9.62E-02	-0.71	1.45E-02
3110035E14Rik	-0.65	9.81E-02	-1.37	3.46E-03
Gm3739	-0.65	1.34E-01	-0.65	6.95E-02
Stk32a	-0.63	5.19E-02	-1.81	1.66E-02
AW551984	-0.63	6.08E-02	-0.59	9.32E-02
Ugt8a	-0.63	4.09E-02	-0.71	1.14E-02
Hrk	-0.61	3.65E-01	-0.60	1.16E-01
Clgn	-0.61	1.62E-01	-0.71	4.93E-03
Slc1a1	-0.61	1.18E-01	-1.04	2.88E-02
Rasgrp3	-0.60	3.99E-01	0.61	4.45E-02
Tenm2	-0.59	6.81E-02	-1.07	1.06E-03
Chrm1	-0.58	1.44E-01	-0.69	2.00E-02
Dmbx1	-0.58	3.05E-01	0.87	1.20E-02

Nefl	-0.58	3.33E-01	-0.90	1.76E-02
Kif5c	-0.58	5.28E-02	-0.63	4.11E-03
Cdo1	0.63	2.51E-01	-0.94	9.17E-04
Tnfaip2	0.67	2.87E-01	-0.59	8.87E-02
Dscaml1	0.68	2.90E-01	-0.91	1.83E-03
Plp1	0.71	2.04E-01	-0.70	4.63E-03
Junb	0.78	3.92E-02	0.86	3.27E-02
Ky	1.08	3.30E-02	0.68	6.99E-02
Thy1	1.14	3.93E-02	0.67	3.19E-02
Selenbp1	1.14	5.20E-02	-0.61	5.45E-02
Agt	1.16	1.56E-01	1.11	1.61E-04
Cacng5	1.19	1.06E-02	0.72	1.25E-02
Als2cl	1.21	2.22E-02	0.69	5.20E-04
Sox10	1.25	5.10E-02	-1.29	1.01E-01
Six3os1	1.47	3.79E-01	-1.07	6.03E-01
Slc30a10	1.57	4.68E-02	-0.62	3.63E-02
Ndrg2	1.67	1.42E-01	-1.05	1.17E-02
Emp1	2.04	9.43E-02	-0.71	1.02E-02
Gm9855	6.76	7.57E-111	6.92	7.96E-214

Table S2: Differentially expressed genes in *E47-/-* primary embryonic NSCs having an E2A binding site in WT cells. Depicted are the results from RNA-Seq indicating the fold-change in gene expression as log2 (log2FC), variance between triplicates as P or Benjamin-Hochberg adjusted P value (adjP).

ensembl	log2FC	P	adjP	Symbol
ENSMUSG00000034674	-1.75	5.15E-45	3.31E-41	Tdg
ENSMUSG00000063320	-1.07	3.65E-05	4.26E-02	1190007I07Rik
ENSMUSG00000043635	-1.06	4.05E-04	2.89E-01	Adamts3
ENSMUSG00000001506	-1.05	1.87E-01	9.99E-01	Col1a1
ENSMUSG00000022206	-0.97	1.15E-01	9.99E-01	Npr3
ENSMUSG00000052613	-0.96	3.15E-03	9.20E-01	Pcdh15
ENSMUSG00000063446	-0.90	3.37E-04	2.57E-01	Plppr1
ENSMUSG00000030222	-0.90	3.71E-02	9.99E-01	Rerg
ENSMUSG00000068373	-0.88	7.73E-02	9.99E-01	D430041D05Rik
ENSMUSG00000020000	-0.86	9.05E-02	9.99E-01	Moxd1
ENSMUSG00000029334	-0.85	3.56E-03	9.58E-01	Prkg2
ENSMUSG00000036815	-0.83	2.82E-03	9.20E-01	Dpp10
ENSMUSG00000049252	-0.82	1.26E-03	6.72E-01	Lrp1b
ENSMUSG00000030854	-0.80	3.94E-03	9.68E-01	Ptpn5
ENSMUSG00000041670	-0.76	3.05E-03	9.20E-01	Rims1
ENSMUSG00000066842	-0.72	5.81E-02	9.99E-01	Hmcn1
ENSMUSG00000046500	-0.71	6.18E-02	9.99E-01	Fam19a4
ENSMUSG00000033147	-0.71	1.97E-02	9.99E-01	Slc22a15
ENSMUSG00000020173	-0.70	1.82E-01	9.99E-01	Cobl
ENSMUSG00000005883	-0.69	1.60E-01	9.99E-01	Spo11
ENSMUSG00000026748	-0.68	1.07E-06	2.75E-03	Plxdc2
ENSMUSG00000071424	-0.67	1.08E-01	9.99E-01	Grid2
ENSMUSG00000063434	-0.67	8.20E-03	9.99E-01	Sorcs3
ENSMUSG00000064293	-0.67	2.14E-02	9.99E-01	Cntn4
ENSMUSG00000020181	-0.67	1.41E-02	9.99E-01	Nav3
ENSMUSG00000067028	-0.66	2.16E-02	9.99E-01	Cntnap5b
ENSMUSG00000047261	-0.66	1.43E-01	9.99E-01	Gap43
ENSMUSG00000053825	-0.65	9.62E-02	9.99E-01	Ppfia2
ENSMUSG00000008658	-0.65	2.75E-01	9.99E-01	Rbfox1
ENSMUSG00000073805	-0.65	2.57E-02	9.99E-01	Fam196a
ENSMUSG00000030077	-0.64	2.46E-01	9.99E-01	Chl1
ENSMUSG00000056758	-0.64	9.09E-02	9.99E-01	Hmga2
ENSMUSG00000022021	-0.63	3.53E-06	7.56E-03	Diaph3
ENSMUSG00000039954	-0.63	5.19E-02	9.99E-01	Stk32a
ENSMUSG00000000296	-0.62	5.13E-02	9.99E-01	Tpd52l1
ENSMUSG00000037855	-0.62	2.31E-02	9.99E-01	Zfp365
ENSMUSG00000044770	-0.61	2.91E-01	9.99E-01	Scml4

ENSMUSG00000022894	-0.61	5.00E-02	9.99E-01	Adamts5
ENSMUSG00000009628	-0.61	2.01E-01	9.99E-01	Tex15
ENSMUSG00000038168	-0.61	2.26E-01	9.99E-01	P3h2
ENSMUSG00000024935	-0.61	1.18E-01	9.99E-01	Slc1a1
ENSMUSG00000046159	-0.60	1.34E-01	9.99E-01	Chrm3
ENSMUSG00000035150	-0.60	4.34E-03	9.96E-01	Eif2s3x
ENSMUSG00000071042	-0.60	3.99E-01	9.99E-01	Rasgrp3
ENSMUSG00000032024	-0.60	6.52E-02	9.99E-01	Clmp
ENSMUSG00000049336	-0.59	6.81E-02	9.99E-01	Tenm2
ENSMUSG00000030022	-0.59	1.11E-01	9.99E-01	Adamts9
ENSMUSG00000026514	-0.59	4.56E-02	9.99E-01	Cnih3
ENSMUSG00000079410	-0.59	1.96E-01	9.99E-01	Gm2897
ENSMUSG00000026764	-0.58	5.28E-02	9.99E-01	Kif5c
ENSMUSG00000035342	0.58	2.35E-02	9.99E-01	Lzts2
ENSMUSG00000031661	0.58	2.37E-01	9.99E-01	Nkd1
ENSMUSG00000035547	0.58	1.16E-01	9.99E-01	Capn5
ENSMUSG00000044164	0.59	2.09E-01	9.99E-01	Rnf182
ENSMUSG00000035891	0.59	1.63E-01	9.99E-01	Cerk
ENSMUSG00000020263	0.59	1.69E-01	9.99E-01	Appl2
ENSMUSG00000026923	0.60	5.18E-02	9.99E-01	Notch1
ENSMUSG00000044197	0.60	2.55E-01	9.99E-01	Gpr146
ENSMUSG00000020893	0.60	1.34E-01	9.99E-01	Per1
ENSMUSG00000022425	0.60	2.70E-01	9.99E-01	Enpp2
ENSMUSG00000047085	0.60	4.94E-02	9.99E-01	Lrrc4b
ENSMUSG00000018451	0.61	1.49E-01	9.99E-01	6330403K07Rik
ENSMUSG00000046961	0.61	3.23E-01	9.99E-01	Gpr156
ENSMUSG00000037003	0.61	1.17E-01	9.99E-01	Tns2
ENSMUSG00000039095	0.61	1.25E-01	9.99E-01	En2
ENSMUSG00000022122	0.61	1.92E-01	9.99E-01	Ednrb
ENSMUSG00000055652	0.61	6.88E-02	9.99E-01	Klhl25
ENSMUSG00000030986	0.61	9.15E-02	9.99E-01	Dhx32
ENSMUSG00000068099	0.61	2.87E-01	9.99E-01	1500009C09Rik
ENSMUSG00000029723	0.61	1.40E-01	9.99E-01	Tsc22d4
ENSMUSG00000032204	0.61	2.11E-01	9.99E-01	Aqp9
ENSMUSG00000048001	0.62	6.11E-02	9.99E-01	Hes5
ENSMUSG00000021250	0.62	1.23E-01	9.99E-01	Fos
ENSMUSG00000044786	0.62	1.31E-01	9.99E-01	Zfp36
ENSMUSG00000021806	0.62	2.21E-02	9.99E-01	Nid2
ENSMUSG00000028756	0.62	1.40E-01	9.99E-01	Pink1
ENSMUSG00000021453	0.62	8.16E-02	9.99E-01	Gadd45g
ENSMUSG00000029049	0.62	8.53E-02	9.99E-01	Morn1
ENSMUSG00000036306	0.62	1.66E-01	9.99E-01	Lzts1
ENSMUSG00000015090	0.62	6.85E-02	9.99E-01	Ptgds
ENSMUSG00000040260	0.63	2.14E-01	9.99E-01	Daam2
ENSMUSG00000030790	0.63	1.41E-01	9.99E-01	Adm
ENSMUSG00000000794	0.63	3.09E-01	9.99E-01	Kcnn3
ENSMUSG00000026227	0.63	1.47E-01	9.99E-01	2810459M11Rik

ENSMUSG00000002908	0.63	1.77E-01	9.99E-01	Kcnn1
ENSMUSG00000056204	0.63	1.18E-01	9.99E-01	Pgpep1
ENSMUSG00000022565	0.63	1.24E-01	9.99E-01	Plec
ENSMUSG00000032269	0.63	3.09E-01	9.99E-01	Htr3a
ENSMUSG00000034472	0.63	3.61E-01	9.99E-01	Rasd2
ENSMUSG00000032298	0.64	3.12E-02	9.99E-01	Neil1
ENSMUSG00000027333	0.64	1.02E-01	9.99E-01	Smox
ENSMUSG00000024206	0.64	1.07E-02	9.99E-01	Rfx2
ENSMUSG00000037705	0.64	2.24E-01	9.99E-01	Tecta
ENSMUSG00000056938	0.65	5.67E-02	9.99E-01	Acbd4
ENSMUSG00000051703	0.65	1.09E-01	9.99E-01	Tmem198
ENSMUSG00000030337	0.65	1.12E-01	9.99E-01	Vamp1
ENSMUSG00000033083	0.65	1.16E-01	9.99E-01	Tbc1d4
ENSMUSG00000042647	0.66	1.58E-01	9.99E-01	Acad12
ENSMUSG00000021379	0.66	1.47E-01	9.99E-01	Id4
ENSMUSG00000033059	0.66	1.31E-01	9.99E-01	Pygb
ENSMUSG00000023800	0.66	1.63E-01	9.99E-01	Tiam2
ENSMUSG00000027684	0.66	2.05E-01	9.99E-01	Mecom
ENSMUSG00000004415	0.67	1.68E-01	9.99E-01	Col26a1
ENSMUSG00000023990	0.67	4.72E-02	9.99E-01	Tfeb
ENSMUSG00000002409	0.67	1.85E-01	9.99E-01	Dyrk1b
ENSMUSG00000040841	0.67	2.59E-02	9.99E-01	Six5
ENSMUSG00000020297	0.67	1.64E-01	9.99E-01	Nsg2
ENSMUSG00000006205	0.67	1.06E-01	9.99E-01	Htra1
ENSMUSG00000055799	0.67	6.79E-02	9.99E-01	Tcf7l1
ENSMUSG00000058586	0.67	7.10E-02	9.99E-01	Serhl
ENSMUSG00000041351	0.67	5.43E-02	9.99E-01	Rap1gap
ENSMUSG00000032656	0.68	1.96E-01	9.99E-01	March3
ENSMUSG00000069633	0.68	1.63E-01	9.99E-01	Pex11g
ENSMUSG00000042804	0.68	1.86E-01	9.99E-01	Gpr153
ENSMUSG00000032087	0.68	2.90E-01	9.99E-01	Dscaml1
ENSMUSG00000032741	0.69	9.26E-02	9.99E-01	Tpcn1
ENSMUSG00000003436	0.69	1.03E-01	9.99E-01	Dll3
ENSMUSG00000050953	0.69	8.04E-03	9.99E-01	Gja1
ENSMUSG00000020785	0.70	1.42E-01	9.99E-01	Camkk1
ENSMUSG00000005686	0.70	6.05E-02	9.99E-01	Ampd3
ENSMUSG00000044337	0.71	3.65E-01	9.99E-01	Ackr3
ENSMUSG00000021127	0.71	6.95E-02	9.99E-01	Zfp36l1
ENSMUSG00000034227	0.71	3.92E-02	9.99E-01	Foxj1
ENSMUSG00000074170	0.71	8.35E-02	9.99E-01	Plekhf1
ENSMUSG00000030621	0.71	1.91E-01	9.99E-01	Me3
ENSMUSG00000031765	0.72	5.48E-02	9.99E-01	Mt1
ENSMUSG00000058056	0.72	4.01E-02	9.99E-01	Palld
ENSMUSG00000001911	0.73	2.66E-02	9.99E-01	Nfix
ENSMUSG00000043557	0.73	8.60E-02	9.99E-01	Mdga1
ENSMUSG00000046618	0.74	1.58E-01	9.99E-01	Olfml2a
ENSMUSG00000010660	0.74	1.71E-01	9.99E-01	Plcd1

ENSMUSG00000063160	0.74	8.40E-02	9.99E-01	Numbl
ENSMUSG00000049556	0.74	9.13E-02	9.99E-01	Lingo1
ENSMUSG00000055782	0.74	1.21E-01	9.99E-01	Abcd2
ENSMUSG00000001750	0.75	4.08E-02	9.99E-01	Tcirg1
ENSMUSG00000001552	0.75	5.94E-02	9.99E-01	Jup
ENSMUSG00000049608	0.75	8.31E-02	9.99E-01	Gpr55
ENSMUSG00000035357	0.75	6.39E-02	9.99E-01	Pdzrn3
ENSMUSG00000022790	0.75	1.50E-01	9.99E-01	Igsf11
ENSMUSG00000049265	0.76	2.90E-01	9.99E-01	Kcnk3
ENSMUSG00000092274	0.76	1.14E-01	9.99E-01	Neat1
ENSMUSG00000032368	0.76	1.86E-02	9.99E-01	Zic1
ENSMUSG00000027298	0.76	4.17E-02	9.99E-01	Tyro3
ENSMUSG00000016028	0.77	9.62E-02	9.99E-01	Celsr1
ENSMUSG00000022382	0.77	3.07E-01	9.99E-01	Wnt7b
ENSMUSG00000000325	0.79	8.53E-02	9.99E-01	Arvcf
ENSMUSG00000032744	0.79	2.51E-01	9.99E-01	Heyl
ENSMUSG00000006958	0.80	2.65E-02	9.99E-01	Chrd
ENSMUSG00000031983	0.81	9.49E-02	9.99E-01	2310022B05Rik
ENSMUSG00000071604	0.81	1.43E-01	9.99E-01	Fam189a2
ENSMUSG00000036528	0.81	3.22E-01	9.99E-01	Ppfibp2
ENSMUSG00000023913	0.81	3.57E-01	9.99E-01	Pla2g7
ENSMUSG00000004105	0.82	1.24E-01	9.99E-01	Angptl2
ENSMUSG00000020108	0.83	2.67E-01	9.99E-01	Ddit4
ENSMUSG00000030087	0.84	3.11E-01	9.99E-01	Klf15
ENSMUSG00000028927	0.84	2.53E-01	9.99E-01	Padi2
ENSMUSG00000030428	0.84	3.02E-01	9.99E-01	Ttyh1
ENSMUSG00000052135	0.84	1.52E-02	9.99E-01	Foxo6
ENSMUSG00000068299	0.85	1.24E-01	9.99E-01	Nat8f4
ENSMUSG00000060376	0.85	5.58E-02	9.99E-01	Bckdha
ENSMUSG00000041544	0.85	2.57E-02	9.99E-01	Disp3
ENSMUSG00000023885	0.86	2.24E-01	9.99E-01	Thbs2
ENSMUSG00000040659	0.86	2.93E-02	9.99E-01	Efhd2
ENSMUSG00000034614	0.86	1.28E-01	9.99E-01	Pik3ip1
ENSMUSG00000019960	0.87	2.74E-01	9.99E-01	Dusp6
ENSMUSG00000029413	0.88	1.97E-01	9.99E-01	Naaa
ENSMUSG00000024076	0.88	6.08E-02	9.99E-01	Vit
ENSMUSG00000028558	0.88	2.97E-01	9.99E-01	Calr4
ENSMUSG00000047786	0.89	9.87E-05	9.75E-02	Lix1
ENSMUSG00000020591	0.89	1.01E-01	9.99E-01	Ntsr2
ENSMUSG00000057060	0.89	1.77E-01	9.99E-01	Slc35f3
ENSMUSG00000040093	0.90	3.65E-01	9.99E-01	Bmf
ENSMUSG00000027447	0.92	6.95E-02	9.99E-01	Cst3
ENSMUSG00000002346	0.93	9.56E-02	9.99E-01	Slc25a42
ENSMUSG00000032394	0.93	9.59E-02	9.99E-01	Igdcc3
ENSMUSG00000053113	0.93	2.11E-01	9.99E-01	Socs3
ENSMUSG00000047361	0.93	1.33E-01	9.99E-01	Gm973
ENSMUSG00000032268	0.94	1.10E-01	9.99E-01	Tmprss5

ENSMUSG00000030605	0.95	1.93E-01	9.99E-01	Mfge8
ENSMUSG00000036995	0.96	8.24E-02	9.99E-01	Asap3
ENSMUSG00000070509	0.96	2.22E-01	9.99E-01	Rgma
ENSMUSG00000069805	0.96	5.21E-02	9.99E-01	Fbp1
ENSMUSG00000022358	0.97	2.99E-01	9.99E-01	Fbxo32
ENSMUSG00000036611	0.99	7.63E-02	9.99E-01	Eepd1
ENSMUSG00000022438	1.00	4.86E-02	9.99E-01	Parvb
ENSMUSG00000025911	1.00	6.89E-02	9.99E-01	Adhfe1
ENSMUSG00000028919	1.01	5.78E-02	9.99E-01	Arhgef19
ENSMUSG00000034714	1.02	2.17E-01	9.99E-01	Ttyh2
ENSMUSG00000063171	1.03	4.01E-03	9.68E-01	Rps4l
ENSMUSG00000039533	1.03	3.00E-01	9.99E-01	Mmd2
ENSMUSG00000024552	1.04	3.16E-02	9.99E-01	Slc14a2
ENSMUSG00000019359	1.05	6.38E-02	9.99E-01	Gdpd2
ENSMUSG00000018169	1.06	1.76E-02	9.99E-01	Mfng
ENSMUSG00000032556	1.08	1.58E-01	9.99E-01	Bfsp2
ENSMUSG00000035606	1.08	3.30E-02	9.99E-01	Ky
ENSMUSG00000047793	1.09	9.86E-02	9.99E-01	Sned1
ENSMUSG00000019577	1.10	1.84E-01	9.99E-01	Pdk4
ENSMUSG00000071550	1.11	1.77E-01	9.99E-01	Cfap44
ENSMUSG00000026475	1.12	5.18E-03	9.99E-01	Rgs16
ENSMUSG00000057880	1.12	2.40E-01	9.99E-01	Abat
ENSMUSG00000059742	1.13	1.11E-01	9.99E-01	Kcnh7
ENSMUSG00000041771	1.15	8.22E-02	9.99E-01	Slc24a4
ENSMUSG00000028167	1.16	1.06E-01	9.99E-01	Bdh2
ENSMUSG00000030088	1.17	9.51E-03	9.99E-01	Aldh1l1
ENSMUSG00000014846	1.19	2.84E-02	9.99E-01	Tppp3
ENSMUSG00000040373	1.19	1.06E-02	9.99E-01	Cacng5
ENSMUSG00000024227	1.21	1.35E-01	9.99E-01	Pdzph1
ENSMUSG00000040495	1.21	9.03E-02	9.99E-01	Chrm4
ENSMUSG00000046182	1.22	1.86E-01	9.99E-01	Gsg1l
ENSMUSG00000025780	1.26	2.11E-01	9.99E-01	Itih5
ENSMUSG00000034706	1.29	9.17E-02	9.99E-01	Dnaic2
ENSMUSG00000039410	1.31	4.33E-02	9.99E-01	Prdm16
ENSMUSG00000041556	1.32	2.92E-02	9.99E-01	Fbxo2
ENSMUSG00000047935	1.32	7.87E-03	9.99E-01	Gm5607
ENSMUSG00000071847	1.33	1.54E-01	9.99E-01	Apcdd1
ENSMUSG00000017692	1.33	1.03E-01	9.99E-01	Rhbdl3
ENSMUSG00000051041	1.34	2.06E-01	9.99E-01	Olfml1
ENSMUSG00000022494	1.40	8.11E-02	9.99E-01	Shisa9
ENSMUSG00000049555	1.40	2.28E-02	9.99E-01	Tmie
ENSMUSG00000029005	1.42	1.05E-01	9.99E-01	Draxin
ENSMUSG00000027215	1.42	1.67E-01	9.99E-01	Cd82
ENSMUSG00000053846	1.47	4.45E-02	9.99E-01	Lipg
ENSMUSG00000090122	1.48	3.25E-03	9.28E-01	Kcne1l
ENSMUSG00000054477	1.48	2.30E-01	9.99E-01	Kcnn2
ENSMUSG00000021933	1.49	5.24E-02	9.99E-01	Gucy1b2

ENSMUSG00000024197	1.54	7.38E-03	9.99E-01	Plin3
ENSMUSG00000026614	1.57	4.68E-02	9.99E-01	Slc30a10
ENSMUSG00000007279	1.61	6.41E-02	9.99E-01	Scube2
ENSMUSG00000042607	1.81	8.73E-03	9.99E-01	Asb4
ENSMUSG00000030208	2.04	9.43E-02	9.99E-01	Emp1
ENSMUSG00000021848	2.73	9.92E-02	9.99E-01	Otx2

Table S3: Differentially expressed genes in *E12-/-* primary embryonic NSCs having an E2A binding site in WT cells. Depicted are the results from RNA-Seq indicating the fold-change in gene expression as log2 (log2FC), variance between triplicates as P or Benjamin-Hochberg adjusted P value (adjP).

ensembl	log2FC	P	adjP	Symbol
ENSMUSG00000001506	-1.85	6.19E-13	1.91E-09	Col1a1
ENSMUSG00000039954	-1.81	1.66E-02	3.60E-01	Stk32a
ENSMUSG00000034674	-1.64	1.39E-120	8.59E-117	Tdg
ENSMUSG00000020000	-1.45	5.06E-03	2.35E-01	Moxd1
ENSMUSG00000005883	-1.43	6.96E-06	4.77E-03	Spo11
ENSMUSG00000023236	-1.40	2.50E-02	4.15E-01	Scg5
ENSMUSG00000029231	-1.35	7.45E-03	2.77E-01	Pdgfra
ENSMUSG00000052613	-1.32	7.25E-03	2.75E-01	Pcdh15
ENSMUSG00000030302	-1.31	2.77E-02	4.30E-01	Atp2b2
ENSMUSG00000043753	-1.27	5.40E-03	2.40E-01	Dmrta1
ENSMUSG00000036815	-1.20	1.43E-01	6.85E-01	Dpp10
ENSMUSG00000062760	-1.15	1.46E-03	1.32E-01	1810041L15Rik
ENSMUSG00000027584	-1.13	2.56E-03	1.73E-01	Oprl1
ENSMUSG00000049336	-1.07	1.06E-03	1.08E-01	Tenm2
ENSMUSG00000069763	-1.07	1.26E-02	3.34E-01	Tmem100
ENSMUSG00000044519	-1.06	8.86E-06	5.21E-03	Zfp488
ENSMUSG00000024935	-1.04	2.88E-02	4.34E-01	Slc1a1
ENSMUSG00000023011	-1.04	4.30E-02	5.04E-01	Faim2
ENSMUSG00000005672	-1.01	1.67E-02	3.60E-01	Kit
ENSMUSG00000063320	-1.00	3.40E-04	5.86E-02	1190007I07Rik
ENSMUSG00000018537	-0.99	5.53E-02	5.49E-01	Pcgf2
ENSMUSG00000028655	-0.99	7.73E-02	5.93E-01	Mfsd2a
ENSMUSG00000063446	-0.97	1.57E-04	3.65E-02	Plppr1
ENSMUSG00000022367	-0.97	1.88E-04	3.99E-02	Has2
ENSMUSG00000030854	-0.97	2.86E-03	1.80E-01	Ptpn5
ENSMUSG00000031285	-0.92	6.14E-02	5.58E-01	Dcx
ENSMUSG00000032087	-0.91	1.83E-03	1.43E-01	Dscaml1
ENSMUSG00000024347	-0.87	1.28E-02	3.36E-01	Psd2
ENSMUSG00000025429	-0.84	1.55E-03	1.35E-01	Pstpip2
ENSMUSG00000050908	-0.84	9.49E-02	6.28E-01	Tvp23a
ENSMUSG00000043635	-0.84	9.06E-12	2.24E-08	Adamts3
ENSMUSG00000005125	-0.83	8.56E-02	6.10E-01	Ndrg1
ENSMUSG00000028626	-0.83	1.08E-02	3.17E-01	Col9a2
ENSMUSG00000026547	-0.78	4.11E-02	4.96E-01	Tagln2
ENSMUSG00000035105	-0.77	1.64E-01	7.09E-01	Egln3
ENSMUSG00000041073	-0.76	1.53E-02	3.51E-01	Nacad
ENSMUSG00000010505	-0.76	6.15E-02	5.58E-01	Myt1

ENSMUSG00000067028	-0.74	9.49E-03	3.11E-01	Cntnap5b
ENSMUSG00000028358	-0.74	6.49E-04	8.47E-02	Zfp618
ENSMUSG00000074607	-0.74	1.30E-03	1.23E-01	Tox2
ENSMUSG00000018865	-0.74	5.21E-02	5.37E-01	Sult4a1
ENSMUSG00000048978	-0.74	1.43E-02	3.46E-01	Nrsn1
ENSMUSG00000022044	-0.74	1.43E-01	6.85E-01	Stmn4
ENSMUSG00000062591	-0.73	7.49E-03	2.78E-01	Tubb4a
ENSMUSG00000037625	-0.73	1.22E-02	3.31E-01	Cldn11
ENSMUSG00000027419	-0.72	9.94E-02	6.34E-01	Pcsk2
ENSMUSG00000040606	-0.72	9.31E-03	3.08E-01	Kazn
ENSMUSG00000038457	-0.72	1.92E-02	3.80E-01	Tmem255b
ENSMUSG00000020034	-0.72	3.57E-04	5.86E-02	Tcp11l2
ENSMUSG00000022346	-0.72	2.63E-01	7.81E-01	Myc
ENSMUSG00000053825	-0.71	1.45E-02	3.46E-01	Ppfia2
ENSMUSG00000030208	-0.71	1.02E-02	3.16E-01	Emp1
ENSMUSG00000021451	-0.70	6.32E-02	5.59E-01	Sema4d
ENSMUSG00000028137	-0.70	2.57E-02	4.24E-01	Celf3
ENSMUSG00000035778	-0.69	1.01E-01	6.34E-01	Ggta1
ENSMUSG00000026778	-0.68	7.45E-06	4.84E-03	Prkcq
ENSMUSG00000024500	-0.67	3.55E-04	5.86E-02	Ppp2r2b
ENSMUSG00000020173	-0.67	3.18E-02	4.50E-01	Cobl
ENSMUSG00000028128	-0.67	3.16E-06	2.44E-03	F3
ENSMUSG00000037754	-0.67	2.68E-04	5.11E-02	Ppp1r16b
ENSMUSG00000041261	-0.67	1.02E-06	1.05E-03	Car8
ENSMUSG00000049612	-0.67	6.93E-05	2.19E-02	Omg
ENSMUSG00000062110	-0.66	3.78E-05	1.41E-02	Scfd2
ENSMUSG00000015829	-0.66	3.32E-03	1.94E-01	Tnr
ENSMUSG00000032425	-0.65	1.03E-02	3.16E-01	Zfp949
ENSMUSG00000037664	-0.65	9.26E-05	2.60E-02	Cdkn1c
ENSMUSG00000038068	-0.64	2.68E-02	4.26E-01	Rnf144b
ENSMUSG00000023341	-0.64	1.39E-02	3.42E-01	Mx2
ENSMUSG00000021696	-0.63	3.31E-02	4.52E-01	Elovl7
ENSMUSG00000026764	-0.63	4.11E-03	2.12E-01	Kif5c
ENSMUSG00000026442	-0.63	3.08E-02	4.47E-01	Nfasc
ENSMUSG00000031673	-0.62	1.75E-03	1.42E-01	Cdh11
ENSMUSG00000042751	-0.62	7.94E-05	2.39E-02	Nmnat2
ENSMUSG00000026614	-0.62	3.63E-02	4.72E-01	Slc30a10
ENSMUSG00000056966	-0.61	7.53E-02	5.92E-01	Gjc3
ENSMUSG00000041817	-0.61	2.13E-02	3.97E-01	Fam169a
ENSMUSG00000058966	-0.61	1.55E-02	3.54E-01	Fam57b
ENSMUSG00000021895	-0.61	5.08E-05	1.69E-02	Arhgef3
ENSMUSG00000029053	-0.60	2.78E-02	4.30E-01	Prkcz
ENSMUSG00000031028	-0.60	9.40E-02	6.27E-01	Tub
ENSMUSG00000041607	-0.60	9.96E-02	6.34E-01	Mbp
ENSMUSG00000036800	-0.60	1.58E-01	7.01E-01	Fam135b
ENSMUSG00000060988	-0.59	7.76E-02	5.93E-01	Galnt13
ENSMUSG00000030096	-0.58	9.19E-04	1.03E-01	Slc6a6

ENSMUSG00000032017	-0.58	4.55E-02	5.11E-01	Grik4
ENSMUSG00000087579	0.58	4.52E-02	5.10E-01	1500017E21Rik
ENSMUSG00000083022	0.58	6.86E-02	5.75E-01	Rps15a-ps6
ENSMUSG00000039115	0.59	6.86E-03	2.66E-01	Itga9
ENSMUSG00000029408	0.59	6.08E-02	5.58E-01	Abcb9
ENSMUSG00000078234	0.59	1.17E-01	6.58E-01	Klhdc7a
ENSMUSG00000026131	0.60	1.12E-03	1.10E-01	Dst
ENSMUSG00000071042	0.61	4.45E-02	5.07E-01	Rasgrp3
ENSMUSG00000032193	0.61	1.99E-05	9.43E-03	Ldlr
ENSMUSG00000070047	0.61	4.32E-02	5.04E-01	Fat1
ENSMUSG00000046186	0.61	2.58E-06	2.12E-03	Cd109
ENSMUSG00000031465	0.61	8.55E-04	1.00E-01	Angpt2
ENSMUSG00000029378	0.63	5.93E-02	5.58E-01	Areg
ENSMUSG00000025475	0.63	2.77E-02	4.30E-01	Adgra1
ENSMUSG00000037010	0.63	9.98E-02	6.34E-01	Apln
ENSMUSG00000003032	0.65	3.68E-03	2.04E-01	Klf4
ENSMUSG00000092035	0.65	1.01E-01	6.35E-01	Peg10
ENSMUSG00000064373	0.65	2.40E-01	7.68E-01	Selenop
ENSMUSG00000028780	0.65	7.80E-04	9.39E-02	Sema3c
ENSMUSG00000046743	0.66	2.45E-04	4.87E-02	Fat4
ENSMUSG00000021991	0.67	1.95E-05	9.43E-03	Cacna2d3
ENSMUSG00000035606	0.68	6.99E-02	5.79E-01	Ky
ENSMUSG00000066842	0.69	2.92E-04	5.29E-02	Hmcn1
ENSMUSG00000026628	0.69	2.14E-01	7.45E-01	Atf3
ENSMUSG00000032332	0.69	1.61E-03	1.37E-01	Col12a1
ENSMUSG00000054612	0.69	6.09E-03	2.54E-01	Mgmt
ENSMUSG00000040373	0.72	1.25E-02	3.34E-01	Cacng5
ENSMUSG00000068794	0.74	6.57E-04	8.47E-02	Col28a1
ENSMUSG00000063558	0.75	8.94E-03	3.07E-01	Aox1
ENSMUSG00000022594	0.76	6.04E-11	1.24E-07	Lynx1
ENSMUSG00000032440	0.77	9.77E-04	1.05E-01	Tgfbr2
ENSMUSG00000061808	0.78	5.47E-01	8.99E-01	Ttr
ENSMUSG00000003617	0.80	7.85E-02	5.93E-01	Cp
ENSMUSG00000052854	0.82	1.35E-02	3.38E-01	Nrk
ENSMUSG00000059003	0.84	3.20E-02	4.50E-01	Grin2a
ENSMUSG00000040605	0.87	1.05E-03	1.08E-01	Bace2
ENSMUSG00000040998	0.89	7.89E-06	4.87E-03	Npnt
ENSMUSG00000025582	0.93	2.84E-08	3.90E-05	Nptx1
ENSMUSG00000028214	0.95	2.44E-05	1.01E-02	Gem
ENSMUSG00000027861	0.95	6.64E-03	2.61E-01	Casq2
ENSMUSG00000022330	1.09	3.56E-02	4.67E-01	Osr2
ENSMUSG00000035686	1.12	1.00E-05	5.63E-03	Thrsp
ENSMUSG00000003545	1.14	4.97E-09	7.67E-06	Fosb